NASA Technical Memorandum 84520

Results of Buffet Tests in a Cryogenic Wind Tunnel

Richmond P. Boyden and William G. Johnson, Jr.

SEPTEMBER 1982

NASA

NASA Technical Memorandum 84520

Results of Buffet Tests in a Cryogenic Wind Tunnel

Richmond P. Boyden and William G. Johnson, Jr.
Langley Research Center
Hampton, Virginia

National Aeronautics
and Space Administration

**Scientific and Technical
Information Branch**

1982

SUMMARY

Buffet tests have been made in a cryogenic wind tunnel at subsonic speeds over a range of stagnation temperatures and pressures. Two semispan-wing models were utilized. One model was a slender delta wing with 65° sweep with sharp leading edges. The other model was an unswept wing of aspect ratio 1.5 with a British NPL 9510 airfoil section.

The tests have shown that it is feasible to use the standard dynamic wing-root bending-moment technique in a cryogenic wind tunnel. The results for the delta-wing model indicate the importance of matching the reduced-frequency parameter in model tests for planforms which are sensitive to reduced-frequency parameter if quantitative buffet measurements are required. The unique ability of a pressurized cryogenic wind tunnel to separate the effects of Reynolds number and of static aeroelastic distortion by variations in the tunnel stagnation temperature and pressure has been demonstrated.

INTRODUCTION

The study of techniques suitable for use in making buffet measurements in cryogenic wind tunnels is one of a number of studies in progress at the Langley Research Center in preparation for performing aerodynamic research in the National Transonic Facility (NTF) when it becomes operational. (See ref. 1.) Buffeting can be defined as the structural response of an aircraft or test model to the aerodynamic excitation produced by separated flows. Because buffeting is a separated-flow phenomenon, it is, of course, dependent on Reynolds number. The NTF, with its capability to vary test Reynolds number over a very wide range, will present a unique opportunity for research in the area of buffet testing. The buffet tests described in this paper, which were carried out in the Langley 0.3-Meter Transonic Cryogenic Tunnel (0.3-m TCT), were based primarily on suggestions by Dennis G. Mabey of the Royal Aircraft Establishment at Bedford, England, in a lecture given at Langley. (See ref. 2.) The primary objective of this study was to evaluate at cryogenic temperatures the use of an existing buffet testing technique, namely, the measurement of the dynamic or unsteady wing-root bending moment. (See refs. 3 and 4.) This evaluation was to be done by obtaining comparable dynamic wing-root bending-moment data at both ambient and cryogenic temperatures to validate the technique and the instrumentation. The secondary objectives were to utilize the unique capabilities of the cryogenic pressure tunnel to study the Reynolds number effect on buffeting at constant dynamic pressure and to study the effect of model aeroelastic distortion on buffeting at constant Reynolds number.

Two buffet semispan-wing models similar to those suggested in reference 2 were constructed and instrumented for these tests. One model was a slender, sharp-leading-edge delta wing with 65° leading-edge sweep known to be relatively insensitive to variations in Reynolds number. (See ref. 5.) This configuration was chosen to provide a base-line model to demonstrate the test technique over the temperature range in a cryogenic wind tunnel. Some buffet measurements on two 65°-swept delta wings are described in reference 5. The other model was an unswept wing of aspect ratio 1.5 with a British NPL 9510 airfoil section (ref. 6) which was expected to be very sensitive to variations in Reynolds number. (See ref. 7.) (This model will be

referred to herein as the NPL 9510 wing model.) The semispan-wing models were cantilevered from a turntable located in the sidewall of the two-dimensional test section of the 0.3-m TCT. It is recognized that wall interference effects are present in these test results because of the size of these three-dimensional models relative to the size of the two-dimensional test section as well as the method for mounting the models. However, in evaluating the test technique by comparing ambient and cryogenic results, wall effects are considered unimportant.

Tests were made at subsonic Mach numbers over a range of stagnation pressure from 122 kPa to 586 kPa and of stagnation temperature from 300 K to 100 K. The angle of attack was varied from -4° to 32° for the delta-wing model and from -2° to 18° for the NPL 9510 wing. Measurements were made of both the dynamic and the steady wing-root bending moments. Some preliminary results from these tests at Mach numbers of 0.35 and below were presented in reference 8.

SYMBOLS

$C_{B,d}$ dynamic wing-root bending-moment coefficient, $M_{B,d}/qS\bar{c}$

$C_{B,s}$ steady wing-root bending-moment coefficient, $M_{B,s}/qS\bar{c}$

$\bar{c}$ mean geometric chord, m

f frequency, Hz

K_T wing-root bending-moment strain-gage sensitivity, N-m/(calibration signal)

k reduced frequency parameter, $\omega\bar{c}/V$, rad

M free-stream Mach number

$M_{B,d}$ time-averaged root-mean-square value of dynamic wing-root bending moment, N-m

$M_{B,s}$ steady wing-root bending moment, N-m

p_t stagnation pressure, Pa or atm

q free-stream dynamic pressure, Pa

R Reynolds number based on $\bar{c}$

S reference area of semispan planform, m^2

T_t stagnation temperature, K

V free-stream velocity, m/sec

x distance along tunnel axis measured from center of turntable, cm

α angle of attack, deg

α_{onset} angle of attack for buffet onset, deg

ζ total damping ratio, aerodynamic and structural, percent of critical damping

ρ free-stream density, kg/m^3

ω angular frequency, $2\pi f$, rad/sec

APPARATUS AND PROCEDURE

Wind Tunnel

The Langley 0.3-Meter Transonic Cryogenic Tunnel (0.3-m TCT) is a single-return, fan-driven wind tunnel which utilizes nitrogen as the test gas. The two-dimensional test section presently installed in the tunnel circuit is 20.3 cm wide and 61.0 cm high. For this investigation, the test section had a slotted floor, a slotted ceiling, and solid sidewalls. A motor-driven turntable that is 22.8 cm in diameter is centrally located in each sidewall for the mounting of two-dimensional airfoil models. The Mach number capability with the two-dimensional test section is from about 0.05 to 0.95. Stagnation pressure can be varied from about 122 kPa to about 608 kPa (1.2 atm to about 6.0 atm), and the stagnation-temperature range is from about 77 K to 327 K. Additional information on the cryogenic-tunnel concept and on the operating characteristics of the 0.3-m TCT is contained in references 1, 9, and 10.

Models

The two buffet semispan-wing models were constructed from the same type of aluminum alloy, 7075-T6, as the turntable to which they were mounted. This was done to minimize the effects of thermal expansion and contraction over the range of test temperatures in order to provide a model mounting as rigid as possible to keep the structural damping to a minimum. The mounting block at the root chord of each wing fits into a recessed cavity on the windward side of the turntable, and it was held in place by screws through the turntable with the threads in the mounting block. A square area about 1.9 cm on a side and 0.08 cm deep was machined into the upper and lower surfaces of the models near the root chord for placement of the root bending-moment strain-gage bridge. A strain-gage bridge and two thermocouples were bonded with cement into the machined recesses. The remaining void was then filled to the original surface with the same cement which is rated for use over the temperature range of interest from 100 K to 300 K. No artificial transition was used to trip the boundary layer on either of the models during these tests. A sketch of the models is shown in figure 1, and figure 2 is a photograph of the two models. The model geometric characteristics are listed in table I. A sketch of the test section of the 0.3-m TCT is shown in figure 3 and photographs of the models mounted in the 0.3-m TCT are shown as figures 4 and 5.

Instrumentation

The buffet data system used for these tests is a two-channel integrated unit designed by James W. Lynch of the Langley Instrument Research Division. Each channel of the buffet system includes switch-selectable gain settings from 200 to 20 000, an active low-pass filter, a root-mean-square converter, and an integrator. It may be operated in either an ac or dc mode. The dc mode is normally used for wind-off calibration of the bending-moment strain gage by application of known moments to the wing

with weights. The dc mode is also utilized to measure the wind-on, steady-state root bending moments of the two wings. In the ac mode, the steady or dc voltages are automatically suppressed. The system averages the root-mean-square values of the unsteady voltage signals from the bending-moment strain gage by integrating the signal for a time interval which is preselected from 1 to 99 sec. For this test, an integration time of 20 sec was used. The two-pole, low-pass, active filter is mounted on plug-in boards and is used to limit the frequency content above the range of interest. For this test, the roll-off frequency was set at about 1000 Hz. The unsteady bending-moment signal was recorded on a magnetic tape recorder for later off-line analysis.

Test Procedure

An electromagnetic shaker apparatus was used to determine the natural frequencies of the model wings, but the results obtained were inconsistent. The reason for this is believed to be that the mass of the shaker head was large compared with the mass of the model wings. (See ref. 11.) Consistent results for the first natural frequency in bending were obtained by repeatedly tapping on the wing and measuring the frequency of the output of the bending-moment strain gages on an electronic frequency meter. The natural frequency for the delta-wing model at ambient temperatures is about 492 Hz, whereas the natural frequency for the NPL 9510 wing model at ambient temperatures is about 270 Hz.

Before the actual wind-tunnel test, the models were loaded statically while in an environmental chamber in order to determine the effect of the large temperature range on the strain-gage sensitivity. A calibration of the sensitivity of the root bending-moment strain gage with temperature for the delta-wing model is shown in figure 6. The variation in the sensitivity with temperature was found to be linear and to increase by 21 percent for the delta wing and 24 percent for the NPL 9510 wing over a range of temperature from 300 K to 110 K. This rather large change in sensitivity with temperature is the apparent result of the strain gages not being well matched to the aluminum alloy used for the models. The calibration curve for each of the two models as a function of temperature was used to correct the strain-gage sensitivity in the data-reduction program.

After the wind tunnel had reached the required test conditions and the angle of attack had been set, the gain of the buffet system was adjusted to maximize the output of the unsteady wing-root bending-moment signal without overloading the instrumentation. This signal was monitored with an oscilloscope and a recording oscillograph for amplifier overload and for the allowable input range for the analog tape recorder. The unsteady bending-moment signal was then integrated for the 20-sec time interval chosen for this test and then recorded on the tunnel data-acquisition system. Afterwards, a 30-sec segment of the unsteady signal was recorded on magnetic tape for later analysis. Then, the steady root bending-moment signal was measured and recorded on the tunnel data-acquisition system. The computation and plotting of both the steady and the dynamic wing-root bending-moment coefficients were done on a desk top calculator with an attached plotter for on-line display.

RESULTS AND DISCUSSION

Delta Wing

The range of test conditions for the delta-wing model is shown in figure 7 for a Mach number of 0.35 by the envelope of the Reynolds number and the reduced-frequency-parameter combinations. The stagnation pressure and temperature are indicated along the boundaries of the envelope. The ability to provide this unique envelope with a single model is a result of the ability of the cryogenic tunnel to control velocity and, therefore, to control reduced frequency, for a given Mach number by providing large changes in the speed of sound through changes in operating temperature.

The results of the buffet tests for the delta-wing model are presented in figure 8 with the steady and the dynamic wing-root bending-moment coefficients plotted as a function of the angle of attack. Figure 8(a) is a comparison of the results obtained at a Mach number of 0.35 at temperatures of 300 K and 110 K with the dynamic pressure held constant at 9.6 kPa. The dynamic bending-moment data agree well up to the point of buffet onset where there is a marked change in slope at an angle of attack of about 18° with the curves diverging at the higher angles of attack, an effect which will be discussed later. The occurrence of buffet onset at an angle of attack of 18° correlates well with the results of Wentz and Kohlman in reference 12 for the angle of attack at which the breakdown of the leading-edge vortex reaches the trailing edge of a 65°-swept delta wing. The steady bending-moment data are seen to be in good agreement, which confirms that there is a negligible Reynolds number effect for the delta-wing model. The small difference in the steady bending-moment coefficients at the higher angles of attack is believed to be a result of the model wing being slightly stiffer at the lower temperature and, thus, more resistant to static aeroelastic distortion because of the approximate 6-percent increase in the modulus of elasticity of the 7075-T6 aluminum alloy between 300 K and 110 K. (See ref. 13.)

Figure 8(b) is a comparison of data at ambient and at cryogenic temperatures for $M = 0.35$ with the tunnel stagnation pressure adjusted so that the Reynolds number is constant. The results for the dynamic bending moment are similar to those in the preceding figure, but the steady bending moments appear to show the effect of static model distortion under load as the steady bending-moment coefficient is lower at the same angle of attack for the higher stagnation pressure. Mabey has suggested in reference 14, based on the frequency spectrum of pressure measurements on a different planform, that the large difference in the dynamic bending moment after buffet onset (shown in both figs. 8(a) and 8(b)) is a result of the magnitude of the excitation spectrum increasing with the increase in reduced-frequency parameter associated with the difference in ambient and cryogenic temperatures.

In an effort to match the reduced-frequency parameter k at ambient temperature with the k at a Mach number of 0.35 at cryogenic temperature, the Mach number at ambient temperature was lowered to 0.21, as shown in figure 8(c), in order to make the free-stream velocities the same at ambient and at cryogenic temperatures. The stagnation pressure was also adjusted to keep the dynamic pressure constant. At these low Mach numbers, any Mach number effect should be small. However, the effect of Mach number does appear in the steady bending moment as seen by the different slopes for the data at the Mach numbers of 0.21 and 0.35. Good agreement for the dynamic bending moment was obtained over the entire range of angle of attack with this procedure. This good agreement in the dynamic wing-root bending moment is considered to be verification that the root bending-moment strain-gage technique works satisfactorily at cryogenic temperatures. The variation in the reduced-frequency

parameter, (fig. 8(c)) of 5.71 to 6.01 rad for the ambient and the cryogenic data, respectively, is a result of the frequency of the first natural bending mode increasing with a decrease in temperature because of the previously mentioned increase in modulus of elasticity of the aluminum alloy.

Figure 8(d) is a plot of the results with three different stagnation pressures at a Mach number of about 0.35 and a temperature of 300 K. The reduced frequency parameter is approximately constant. These data also appear to show the effect of model distortion on the steady bending moment as the increased pressure causes a decrease in the coefficient. The decrease in the dynamic bending-moment coefficient seen at the higher angles of attack in figure 8(d) with increased pressure is believed to be a result of the aerodynamic damping increasing with the increase in density. A discussion of the measurement of the damping will be covered in a later section.

Figure 8(e) is a comparison of results for a Mach number of 0.35 at temperatures of 150 K and 110 K at the same stagnation pressure. In an effort to minimize test time, only the points at an angle of attack of 0° and around buffet onset were defined. Good agreement was obtained for both the steady and the dynamic bending moments over the range of Reynolds number.

The test results for a Mach number of 0.60 are shown in figure 8(f) for temperatures of 300 K and 110 K and a constant dynamic pressure of 24.0 kPa. The break which corresponds to the angle of attack for buffet onset is seen to occur at about 22° in both the steady and the dynamic bending-moment data. Also, the break in the curves is seen to be more abrupt at a Mach number of 0.60 than it was at a Mach number of 0.35. The shape of the curve for the dynamic bending-moment coefficient is different after buffet onset in that the curve reaches a peak and then tends to decrease with further increase in angle of attack, rather than continuing to increase with angle of attack. As was the case at the lower Mach number of 0.35 in figure 8(a), the steady bending-moment data in figure 8(f) appear to show that the wing at a temperature of 110 K is stiffer and therefore is more resistant to static aeroelastic distortion than is the same wing at 300 K.

Figure 8(g) compares the test results at a Mach number of 0.60 and a constant Reynolds number at ambient and cryogenic temperatures. These data at a Mach number of 0.60 do not collapse into a single curve which is similar to the results obtained at a Mach number of 0.35 with the Reynolds number held constant in figure 8(b). In the case of the steady bending-moment coefficient, the explanation has to be that the static aeroelastic distortion of the wing results in a decrease in $C_{B,s}$ with an increase in stagnation pressure, or dynamic pressure. The difference in the dynamic bending-moment data is considered to be a result of the difference in the reduced frequency parameter and the resulting difference in the magnitude of the excitation spectrum as previously discussed for the $M = 0.35$ data.

Figure 8(h) shows data taken in an attempt to collapse the dynamic bending-moment coefficient data in a way similar to that in figure 8(c) by adjusting the Mach number and the stagnation pressure so that the reduced-frequency parameter was almost constant and the dynamic pressure was constant. This procedure did not collapse the $C_{B,d}$ curves the way that it did in figure 8(c) because of the apparent Mach number effect on the angle of attack for buffet onset and on the shape of the curve after buffet onset. The Mach number effect is also shown in the steady bending-moment data of figure 8(h). Figure 8(i) shows a comparison of data at a Mach number of 0.60 for two stagnation pressures at ambient temperature. The data at the higher pressures are seen to have the lower steady and dynamic bending-moment coefficients.

As shown in figures 8(j) and 8(k), attempts were also made to obtain data where the dynamic bending-moment coefficients would collapse with data obtained at Mach numbers of 0.70 and 0.85, respectively, by matching the velocity and the dynamic pressure. The data in figure 8(j) did not collapse, presumably because of the apparent Mach number effect on the angle of attack for buffet onset and on the shape of the dynamic-data curve after buffet onset. However, the dynamic bending-moment data in figure 8(k) for Mach numbers of 0.49 and 0.85 did collapse over the limited angle-of-attack range from about 18° to 26°.

The angle of attack at which buffet onset occurred for the delta-wing model as determined by the breakpoint in the dynamic bending-moment coefficient data in figure 8 is plotted as a function of Mach number in figure 9(a). The applicable Reynolds number for each of these same points is shown in figure 9(b). The angle of attack for buffet onset is seen to increase from 18° for Mach numbers from 0.21 to 0.35 to 22° for Mach numbers from 0.49 to 0.85. Reynolds number had no apparent effects on the angle of attack for buffet onset for the delta-wing model as evidenced by the data in figure 9.

NPL 9510 Wing

The steady and the dynamic wing-root bending-moment coefficients as a function of angle of attack for the NPL 9510 wing model are contained in figure 10. Figure 10(a) illustrates the large range of the buffet onset angle of attack from about 8° to 14° as a result of an increase in Reynolds number from 0.78×10^6 to 3.75×10^6 that arises from a variation in the stagnation pressure from 122 kPa to 586 kPa at a stagnation temperature of 300 K. As previously mentioned, this wing was chosen with an airfoil section which should be sensitive to variations in Reynolds number.

Figure 10(b) shows the test results at a Mach number of 0.30 and a constant dynamic pressure of 34.7 kPa with stagnation temperatures of 300 K and 100 K with resultant values of Reynolds number of 3.75×10^6 and 17.35×10^6. In the dynamic bending-moment results, the buffet-onset angle of attack decreases from about 14° to 11° with the increase in Reynolds number. The steady bending-moment results show a break in the curves at angles of attack of about 15° and 11° and are in good agreement at low angles of attack. Figure 10(c) shows a comparison of four runs at a constant dynamic pressure of 28.9 kPa with a range of Reynolds number from 3.12×10^6 to 12.51×10^6. As can be seen in figure 10(d) with the Reynolds number held constant at 3.12×10^6, there is some difference in the slope of the steady bending moment at the lower angles of attack. This difference is thought to be caused by the static aeroelastic distortion of the model wing which is a result of the variation in dynamic pressure. In the dynamic bending moment, there is no apparent change in buffet onset angle of attack and the dynamic bending-moment coefficients are insensitive to variations in the reduced frequency parameter. The agreement in the dynamic bending-moment data in figure 10(d) is again considered to be a verification that the measurement of the wing-root bending moment as a buffet-test technique works satisfactorily at cryogenic temperatures. Adjusting the Mach number and the stagnation pressure in figure 10(e) to match the dynamic pressure and the free-stream velocity did not tend to collapse the dynamic bending-moment curves for the NPL 9510 model as it did for the delta-wing model. The buffet onset angle of attack differed by about 2°. This is thought to be a result of the Reynolds number sensitivity of this airfoil section. Figure 10(f) is a comparison of two runs at a constant stagnation temperature of 110 K for an increase in stagnation pressure from 122 kPa to 488 kPa. The buffet-onset angle of attack decreases from about 13° to about 11.5°.

The results for a Mach number of 0.60 are contained in figures 10(g) to 10(k). In these figures, the dynamic bending-moment coefficient is seen to increase gradually with angle of attack before buffet onset, rather than staying almost flat or constant before buffet onset as was the case at $M = 0.30$. The gradual increase in $C_{B,d}$ makes it more difficult to determine the buffet-onset angle of attack. However, the approximate angle can be determined, for example, in figure 10(g) where the change in slope appears to occur at an angle of attack of about 8°. Figure 10(h) is a comparison of the results for a constant stagnation pressure of 494 kPa at temperatures of 300 K and 110 K. In this figure, the angle of attack for buffet onset is again at about 8°. There is an apparent offset between the steady bending-moment curves. Data for ambient and cryogenic temperatures are shown for the same Reynolds number of 5.63×10^6 in figure 10(i), and both the steady and the dynamic results are in good agreement. The data shown in figure 10(j) were obtained in an attempt to match the reduced-frequency parameter and the dynamic pressure. However, the magnitudes of the dynamic bending-moment coefficients did not match. A comparison of test results at 110 K for two different pressures at $M = 0.60$ is contained in figure 10(k).

The limited amount of data taken at a Mach number of 0.70 is shown in figure 10(l) where the buffet-onset angle of attack appears to be about 7°. Figure 10(m) is a plot of data at 122 kPa and 110 K for Mach numbers of 0.30, 0.60, 0.70, and 0.80. The increase in slope of the steady bending-moment coefficients at the lower angles of attack with increasing Mach number is readily apparent as is the decrease in buffet-onset angle of attack.

The buffet-onset angle of attack taken from figures 10(a) to 10(e) for the NPL 9510 wing model at a Mach number of 0.30 is summarized in figure 11 as a function of Reynolds number. With increasing values of Reynolds number, the angle of attack for buffet onset is seen to rise from about 8° to a peak of about 14° and then to decrease to about 11°.

Damping Measurements

In order to determine the wind-on total damping ratio, aerodynamic and structural, the analog signals recorded on magnetic tape were digitized at 3000 samples per second. About 5 seconds of data at each selected test point were processed by digital analysis techniques. Measurements of the total damping ratio were made from a least-squares fit of the decay of the envelopes of the autocorrelation function. (See ref. 15.) The frequency of oscillation was determined from the average time between peaks of the autocorrelation function. Wind-on values of the total damping ratio for some selected test conditions are listed in tables II and III. These damping-ratio measurements are plotted in figures 12 and 13 along with the wind-off damping-ratio value, and the data points have been fitted with a least-squares straight line. The total damping ratio is seen to vary roughly as the product of the free-stream density and velocity. With the assumption that the structural damping remains constant, the aerodynamic damping component of the total damping would then be proportional to the product of the free-stream density and velocity as pointed out by Mabey in reference 2.

The structural damping of the model wings in still air at ambient temperature was measured from the trace of a recording oscillograph of the decay of an impulsive response. For the delta wing, the damping in still air was about 0.25 percent of critical and for the NPL 9510 wing the damping was about 0.67 percent of critical.

CONCLUSIONS

Buffet tests have been made in a cryogenic wind tunnel over a range of stagnation temperatures and pressures. Two semispan-wing models were utilized. One model was a slender delta wing of 65° sweep with sharp leading edges. The other model was an unswept wing of aspect ratio 1.5 with a British NPL 9510 airfoil section. The following conclusions may be made:

1. It is feasible to use the standard dynamic wing-root bending-moment technique for buffet tests in a cryogenic wind tunnel.

2. The results for the slender delta wing indicate the importance of matching the reduced-frequency parameter in model buffet tests for planforms which are sensitive to reduced-frequency parameter if quantitative buffet measurements are required.

3. It is possible in a pressurized cryogenic wind tunnel to separate the effects of Reynolds number and of static aeroelastic distortion by variations in the tunnel stagnation temperature and pressure.

Langley Research Center
National Aeronautics and Space Administration
Hampton, VA 23665
August 12, 1982

REFERENCES

1. Kilgore, Robert A.: Development of the Cryogenic Tunnel Concept and Application to the U.S. National Transonic Facility. Towards New Transonic Windtunnels, AGARD-AG-240, Nov. 1979, pp. 2-1 - 2-27.

2. Mabey, Dennis G.: Some Remarks on Dynamic Aeroelastic Model Tests in Cryogenic Wind Tunnels. NASA CR-145029, 1975.

3. Davis, Don D., Jr.; and Wornom, Dewey E.: Buffet Tests of an Attack-Airplane Model With Emphasis on Analysis of Data From Wind-Tunnel Tests. NACA RM L57H13, 1958.

4. Ray, Edward J.; and Taylor, Robert T.: Buffet and Static Aerodynamic Characteristics of a Systematic Series of Wings Determined From a Subsonic Wind-Tunnel Study. NASA TN D-5805, 1970.

5. Mabey, D. G.; and Butler, G. F.: Measurements of Buffeting on Two 65° Delta Wings of Different Materials. Unsteady Airloads in Separated and Transonic Flow, AGARD-CP-226, July 1977, pp. 6-1 - 6-14.

6. Hall, D. J.; Quincey, V. G.; and Lock, R. C.: Some Results of Wind-Tunnel Tests of an Aerofoil Section (NPL 9510) Combining a 'Peaky' Upper Surface-Pressure Distribution With Rear Loading. C.P. No. 1292, British A.R.C., 1974.

7. Lock, R. C.; and Fulker, J. L.: Design of Supercritical Aerofoils. Aeronaut. Q., vol. XXV, pt. 4, Nov. 1974, pp. 245-265.

8. Boyden, Richmond P.; and Johnson, William G., Jr.: Preliminary Results of Buffet Tests in a Cryogenic Wind Tunnel. NASA TM-81923, 1981.

9. Kilgore, Robert A.: Design Features and Operational Characteristics of the Langley 0.3-Meter Transonic Cryogenic Tunnel. NASA TN D-8304, 1976.

10. Ray, Edward J.; Ladson, Charles L.; Adcock, Jerry B.; Lawing, Pierce L.; and Hall, Robert M.: Review of Design and Operational Characteristics of the 0.3-Meter Transonic Cryogenic Tunnel. NASA TM-80123, 1979.

11. Bisplinghoff, Raymond L.; Ashley, Holt; and Halfman, Robert L.: Aeroelasticity. Addison-Wesley Pub. Co., Inc., c.1955.

12. Wentz, William H., Jr.; and Kohlman, David L.: Wind Tunnel Investigations of Vortex Breakdown on Slender Sharp-Edged Wings. NASA CR-98737, 1968.

13. Schwartzberg, Fred R.; Osgood, Samuel H.; Herzog, Richard G.; and Knight, Marvin (compiler, AFML): Cryogenic Materials Data Handbook (Revised) 1970, Volume I. AFML-TDR-64-280, Vol. I. (Revised 1970), U.S. Air Force, July 1970. (Available from DTIC as AD 713 619.)

14. Mabey, D. G.: Some Remarks on Buffeting. Tech. Memo. Struct. 980, British R.A.E., Feb. 1981.

15. Cole, Henry A., Jr.: On-the-Line Analysis of Random Vibrations. AIAA Paper No. 68-288, Apr. 1968.

TABLE I.- GEOMETRIC CHARACTERISTICS OF MODEL BASED ON SEMISPAN PLANFORMS

(a) Delta-wing model

Leading-edge sweep, deg	65
Trailing-edge sweep, deg	0
Semispan, cm	9.48
Surface area, cm^2	96.26
Root chord, cm	20.32
Mean geometric chord, cm	13.55
Aspect ratio	0.93
Airfoil section	Flat plate with beveled leading edge

(b) NPL 9510 wing model

Leading-edge sweep, deg	0
Trailing-edge sweep, deg	0
Semispan, cm	15.29
Surface area, cm^2	155.35
Root chord, cm	10.16
Mean geometric chord, cm	10.16
Aspect ratio	1.50
Airfoil section	NPL 9510

TABLE II.- VALUES OF TOTAL DAMPING RATIO FOR DELTA-WING MODEL

M	p_t, kPa	T_t, K	ρ, kg/m^3	V, m/sec	$\frac{\rho V}{(\rho V)_{ref}^*}$	α, deg	f, Hz	ζ, percent
0.35	122	300	1.33	120	0.60	0	495	1.51
						10	495	.74
						20	496	.79
						30	494	1.12
0.35	488	300	5.34	120	2.42	0	493	2.18
						10	495	2.50
						20	492	2.49
						26	490	2.24
						30	486	2.32
0.35	122	110	3.62	73	1.00	0	515	0.84
						10	515	1.42
						20	515	2.07
						26	516	1.75
						30	510	2.17
0.21	320	300	3.63	73	1.00	0	490	1.10
						8	489	1.31
						20	488	1.11
						26	486	1.39
						30	487	1.47

*$(\rho V)_{ref}$ denotes a reference condition at M = 0.35, p_t = 122 kPa, and T_t = 110 K.

TABLE III.- VALUES OF TOTAL DAMPING RATIO FOR NPL 9510 WING MODEL

M	p_t, kPa	T_t, K	ρ, kg/m^3	V, m/sec	$\frac{\rho V}{(\rho V)_{ref}^*}$	α, deg	f, Hz	ζ, percent
0.30	488	300	5.42	103	2.45	0	272	1.80
						10	268	1.43
						15	269	1.40
						18	268	1.47
0.30	122	110	3.68	62	1.00	0	288	1.24
						10	286	
						15	282	.95
						18	283	.83

$^*(\rho V)_{ref}$ denotes a reference condition at M = 0.30, p_t = 122 kPa, and T_t = 110 K.

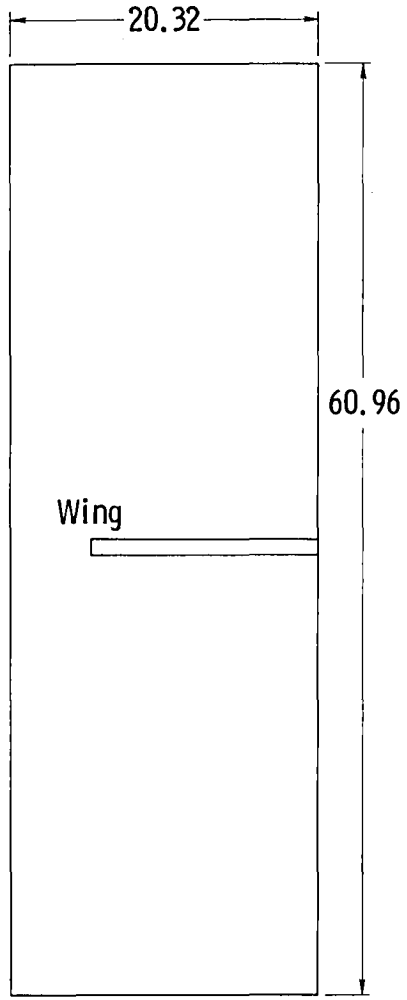

(a) Two-dimensional test section of tunnel.

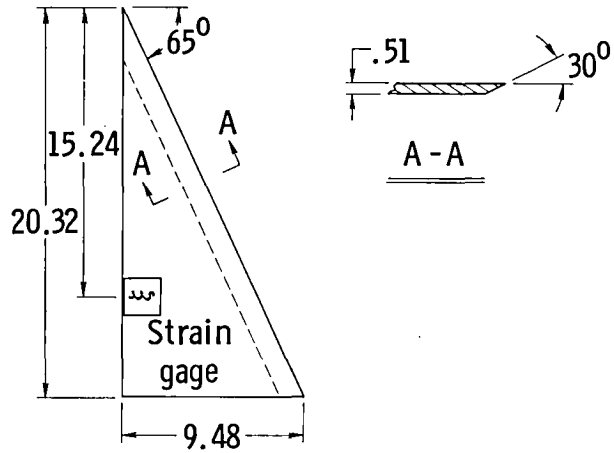

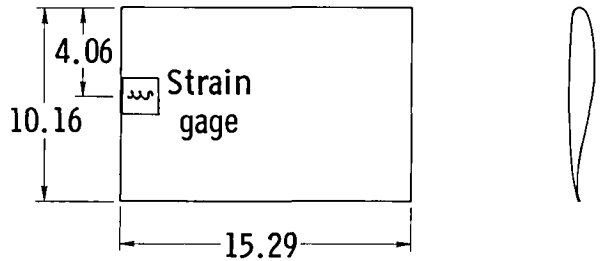

(b) Buffet wings.

Figure 1.- Sketches showing end view of test section of the 0.3-Meter Transonic Cryogenic Tunnel and the buffet models. Linear dimensions are in centimeters.

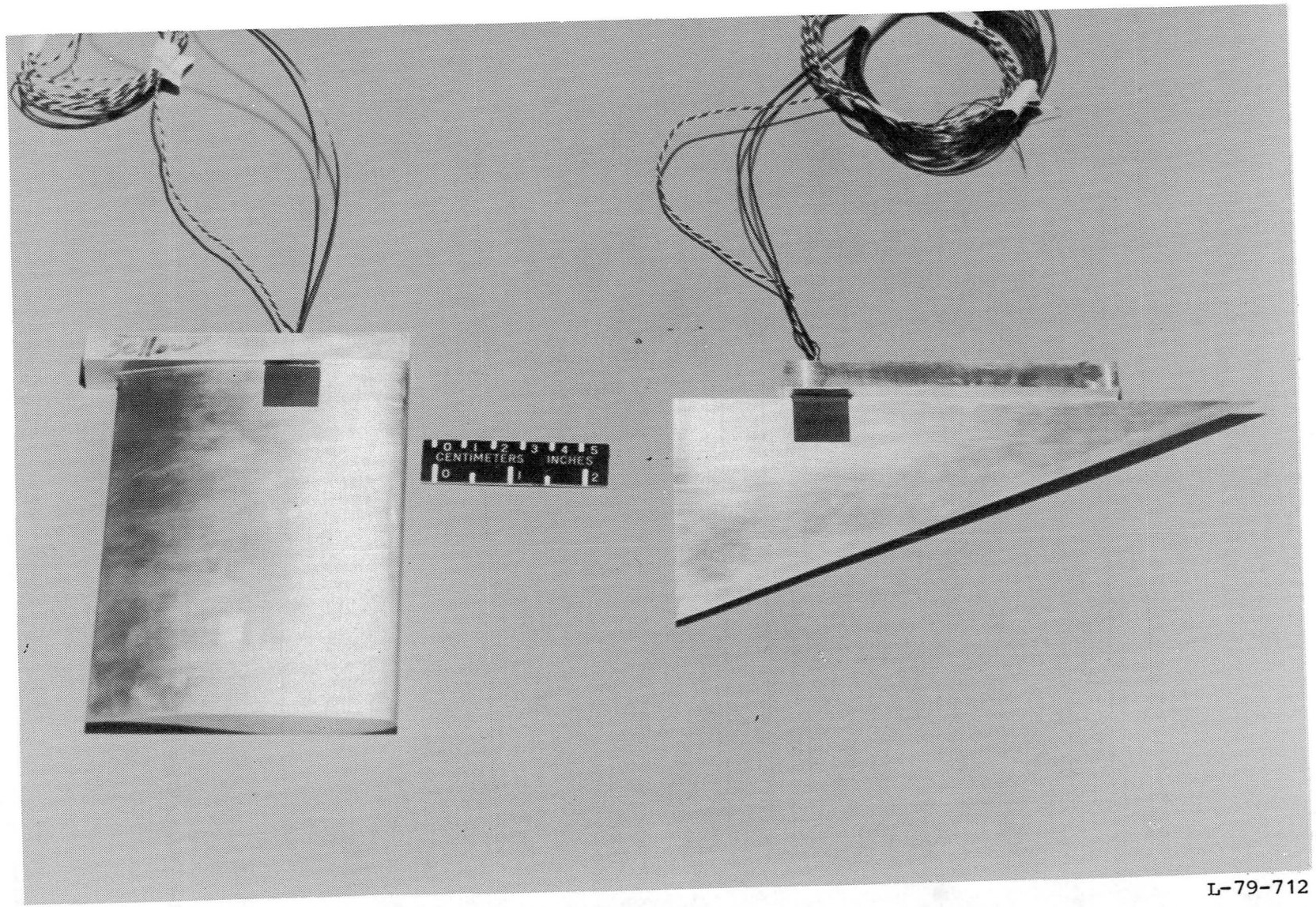

Figure 2.- Photograph of buffet semispan-wing models.

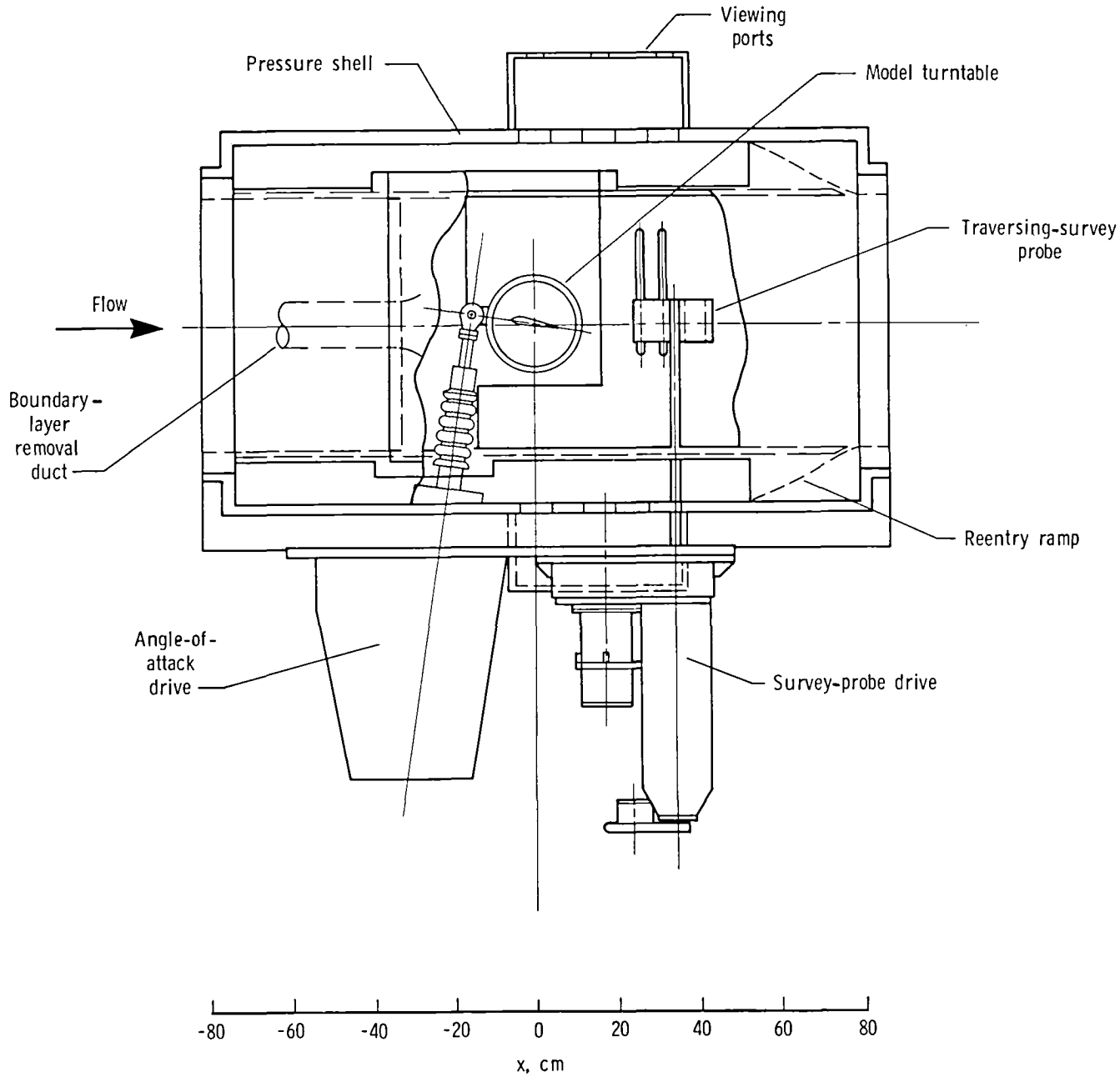

Figure 3.- Sketch of side view of two-dimensional test section of the 0.3-Meter Transonic Cryogenic Tunnel.

L-79-6034

Figure 4.- Photograph of delta-wing buffet model mounted in the 0.3-Meter Transonic Cryogenic Tunnel with slotted floor in background.

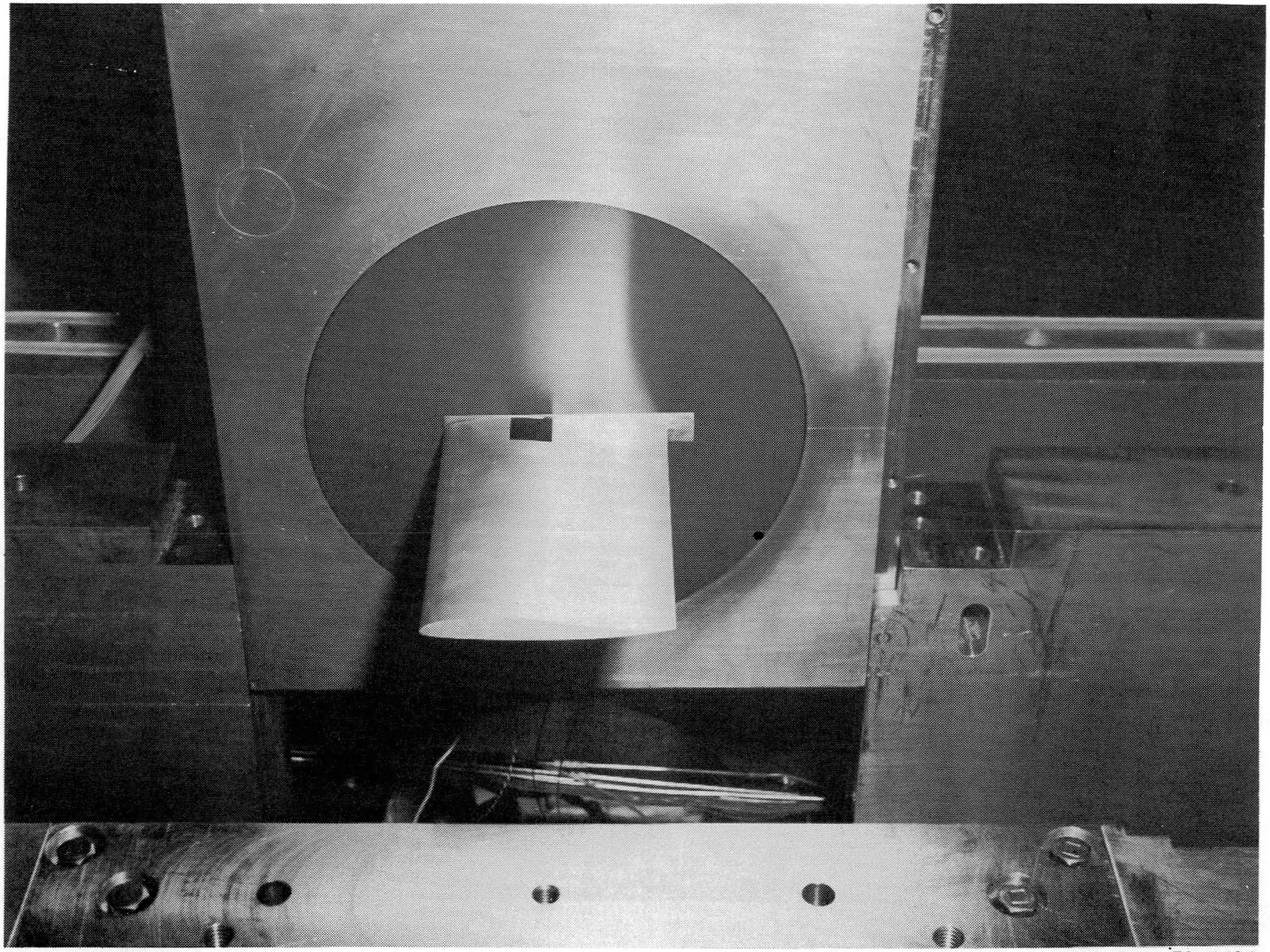

L-79-6696

Figure 5.- Photograph of NPL 9510 wing buffet model mounted on turntable with sidewall insert raised in the 0.3-Meter Transonic Cryogenic Tunnel.

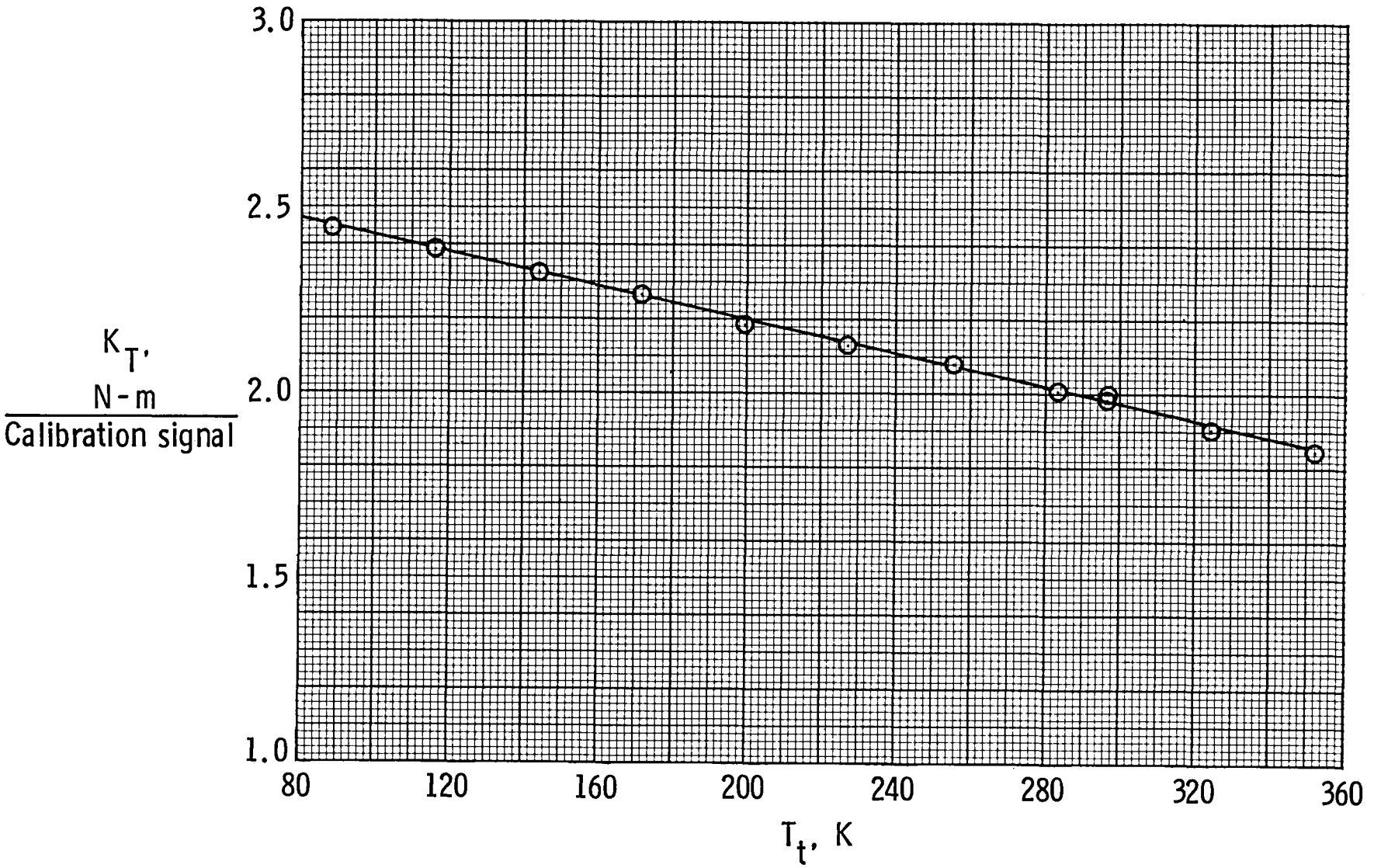

Figure 6.- Effect of temperature on root bending-moment strain-gage sensitivity for delta-wing model.

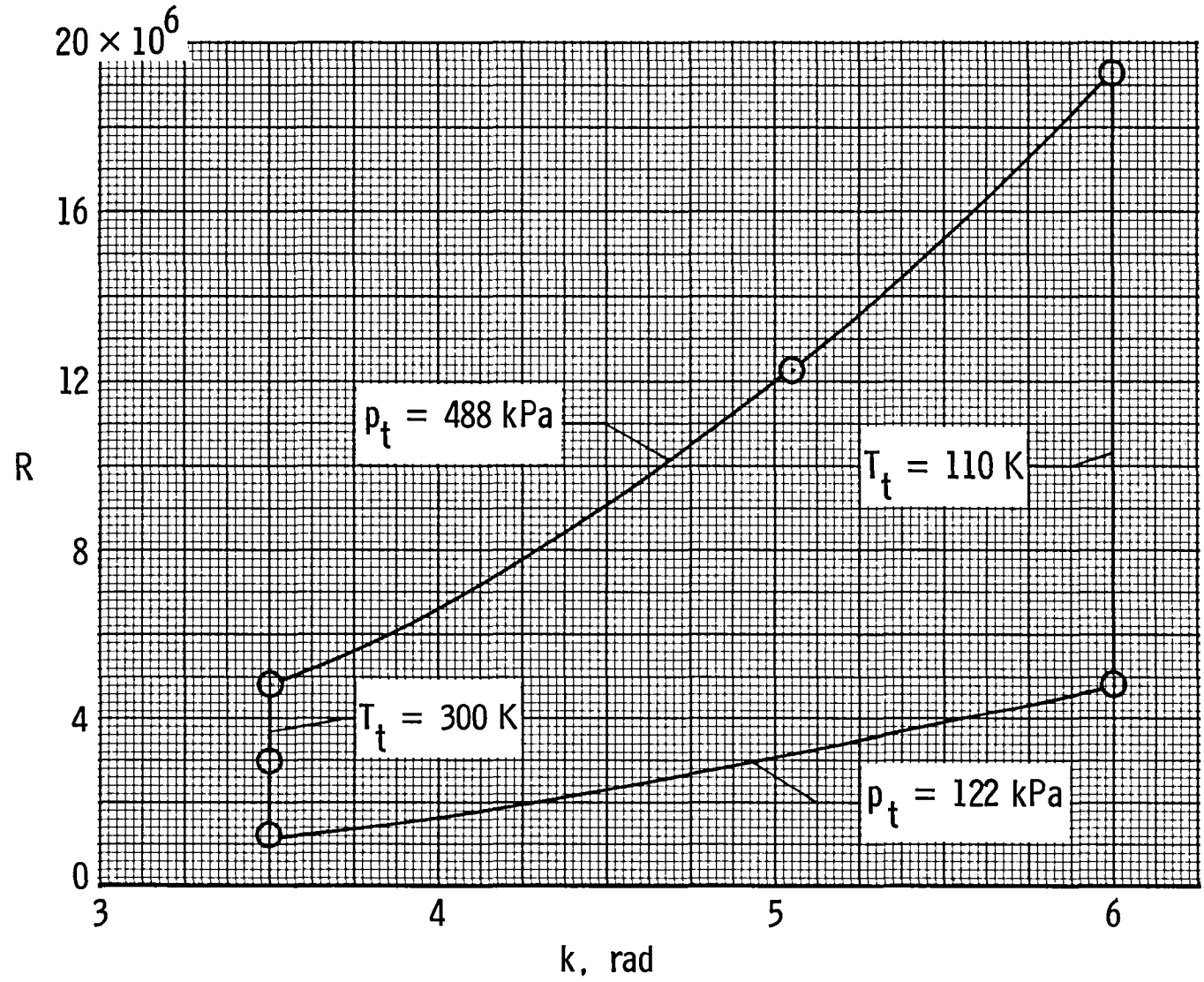

Figure 7.- Buffet-test envelope for delta-wing model in the 0.3-Meter Transonic Cryogenic Tunnel. M = 0.35.

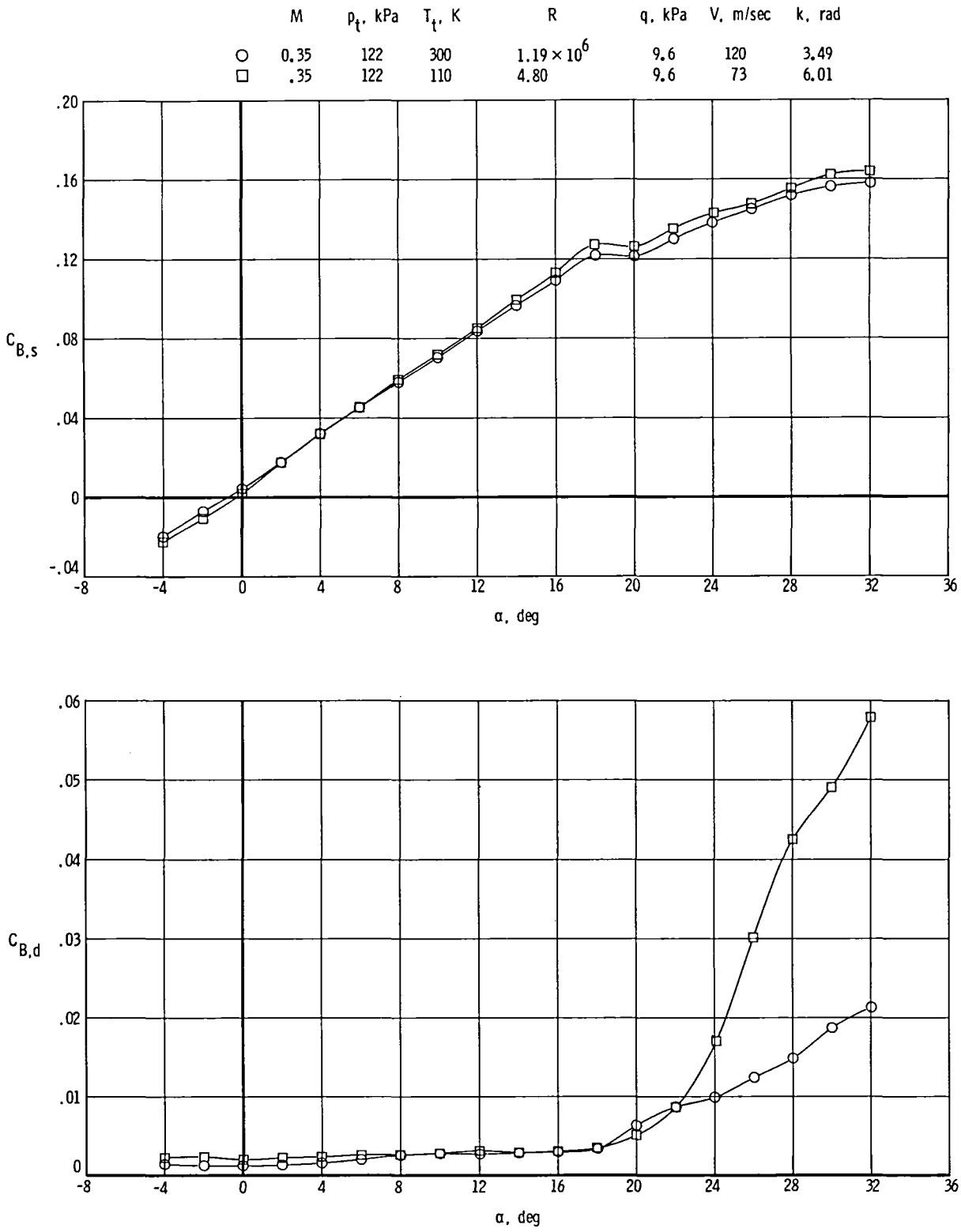

(a) M = 0.35; p_t = 122 kPa.

Figure 8.- Variation of steady and dynamic wing-root bending-moment coefficients with angle of attack for delta-wing model.

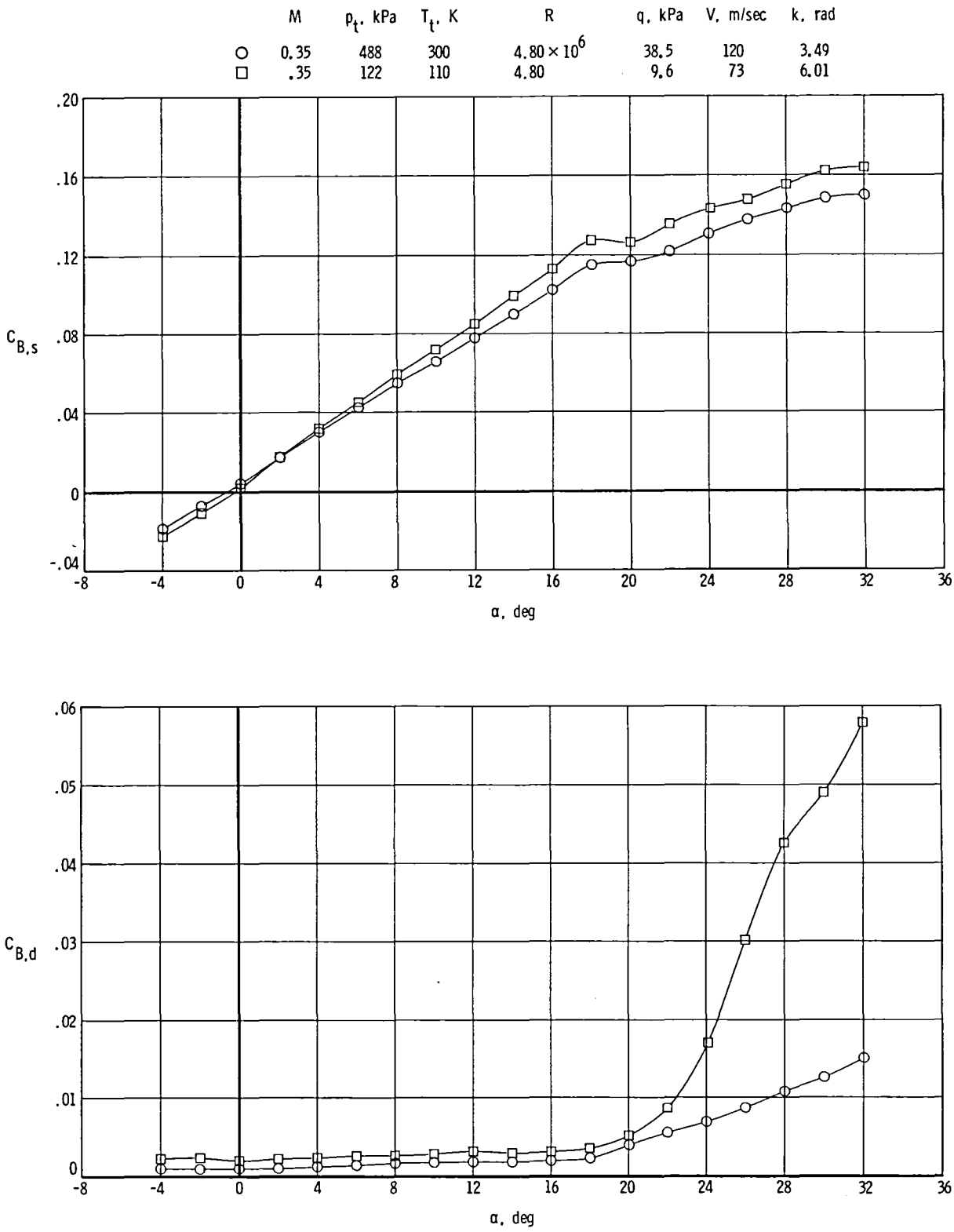

(b) M = 0.35; R = 4.80×10^6.

Figure 8.- Continued.

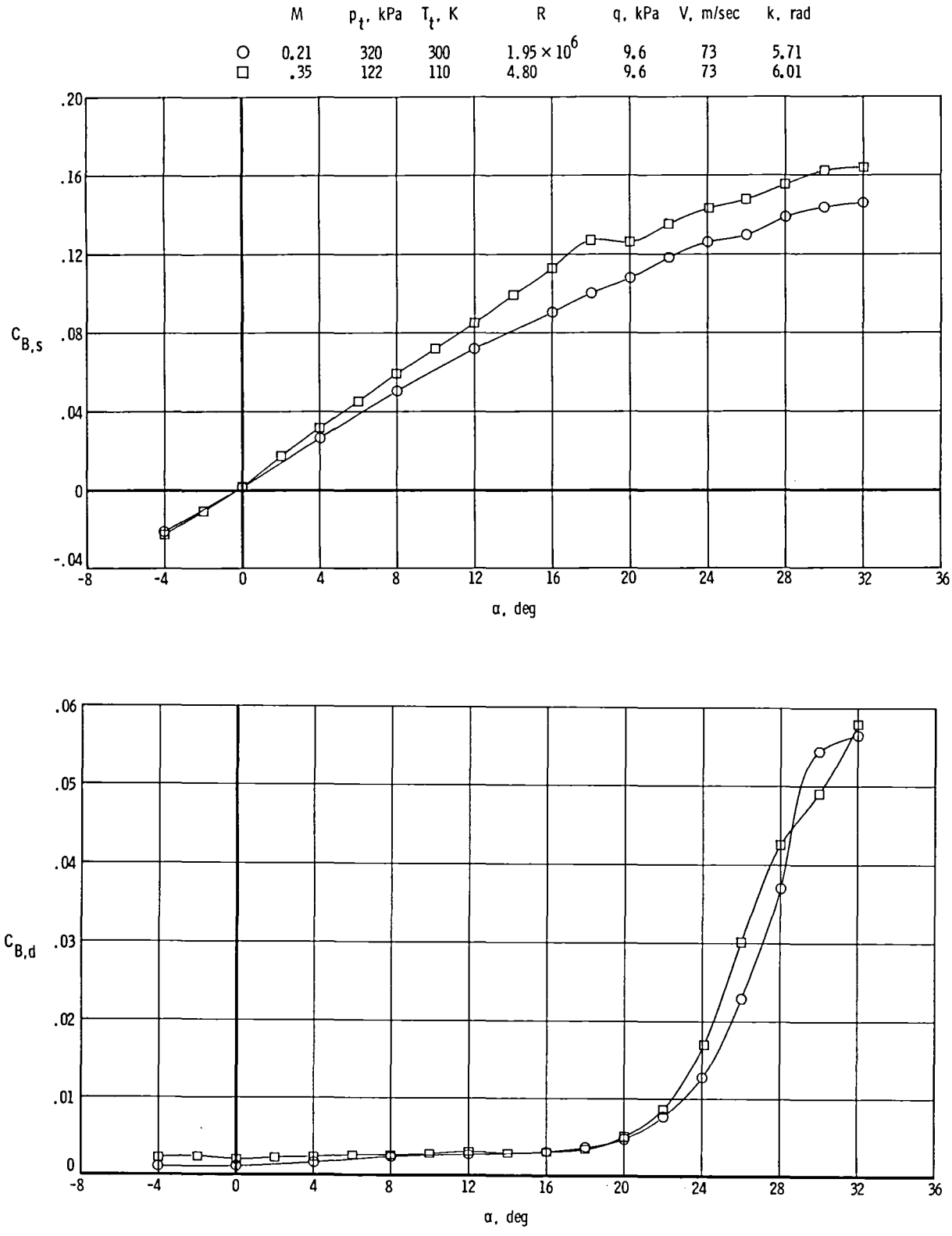

(c) V = 73 m/sec; q = 9.6 kPa.

Figure 8.- Continued.

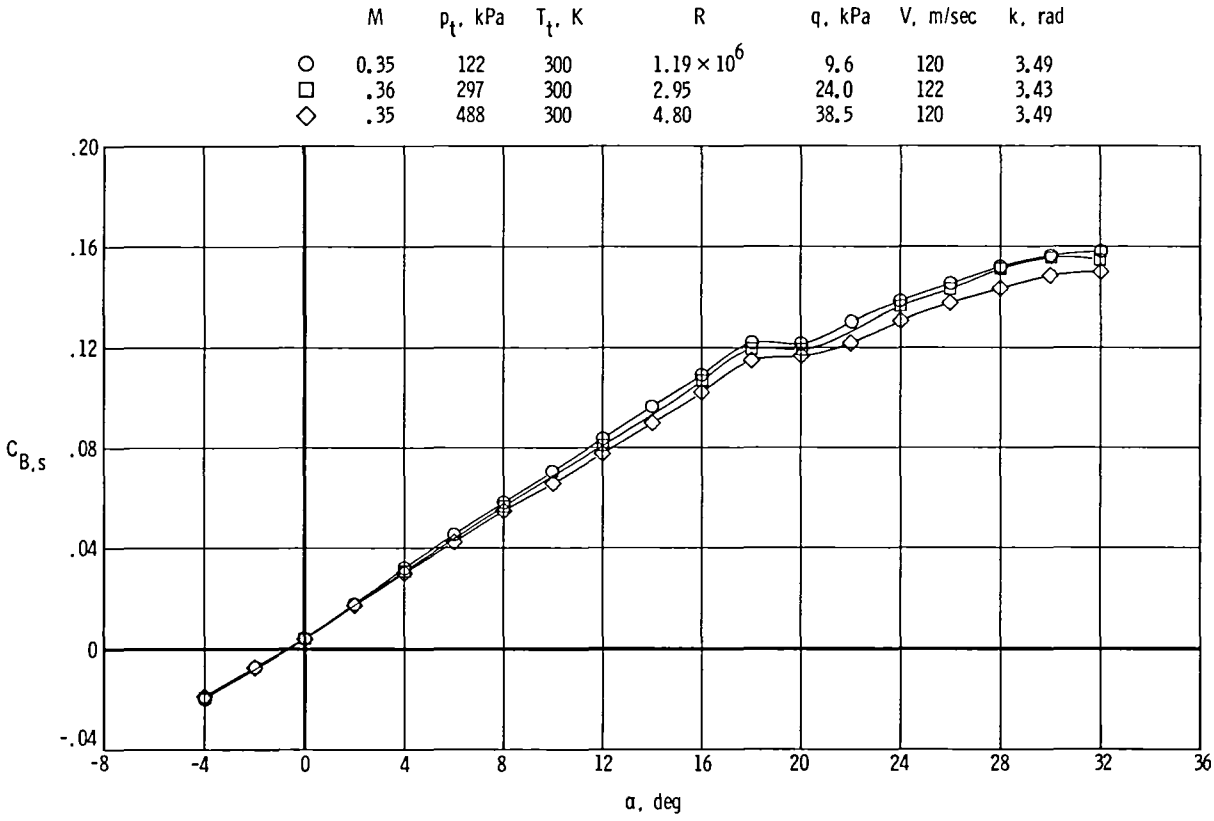

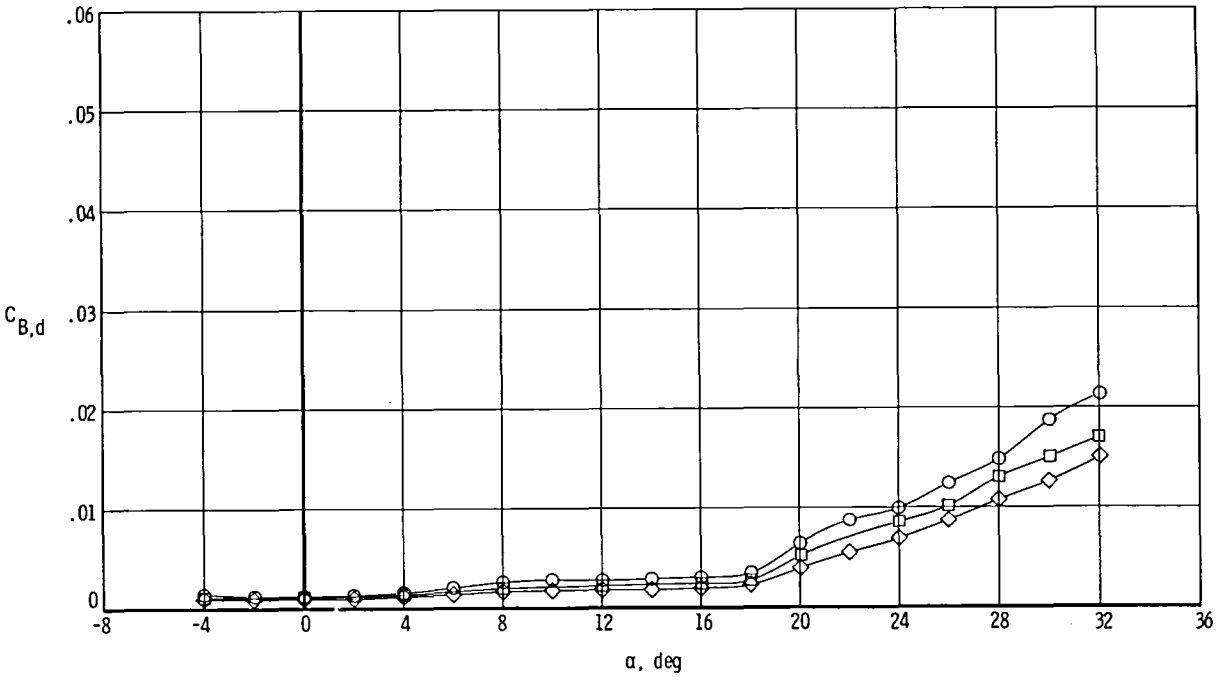

(d) $M \approx 0.35$; $T_t = 300$ K.

Figure 8.- Continued.

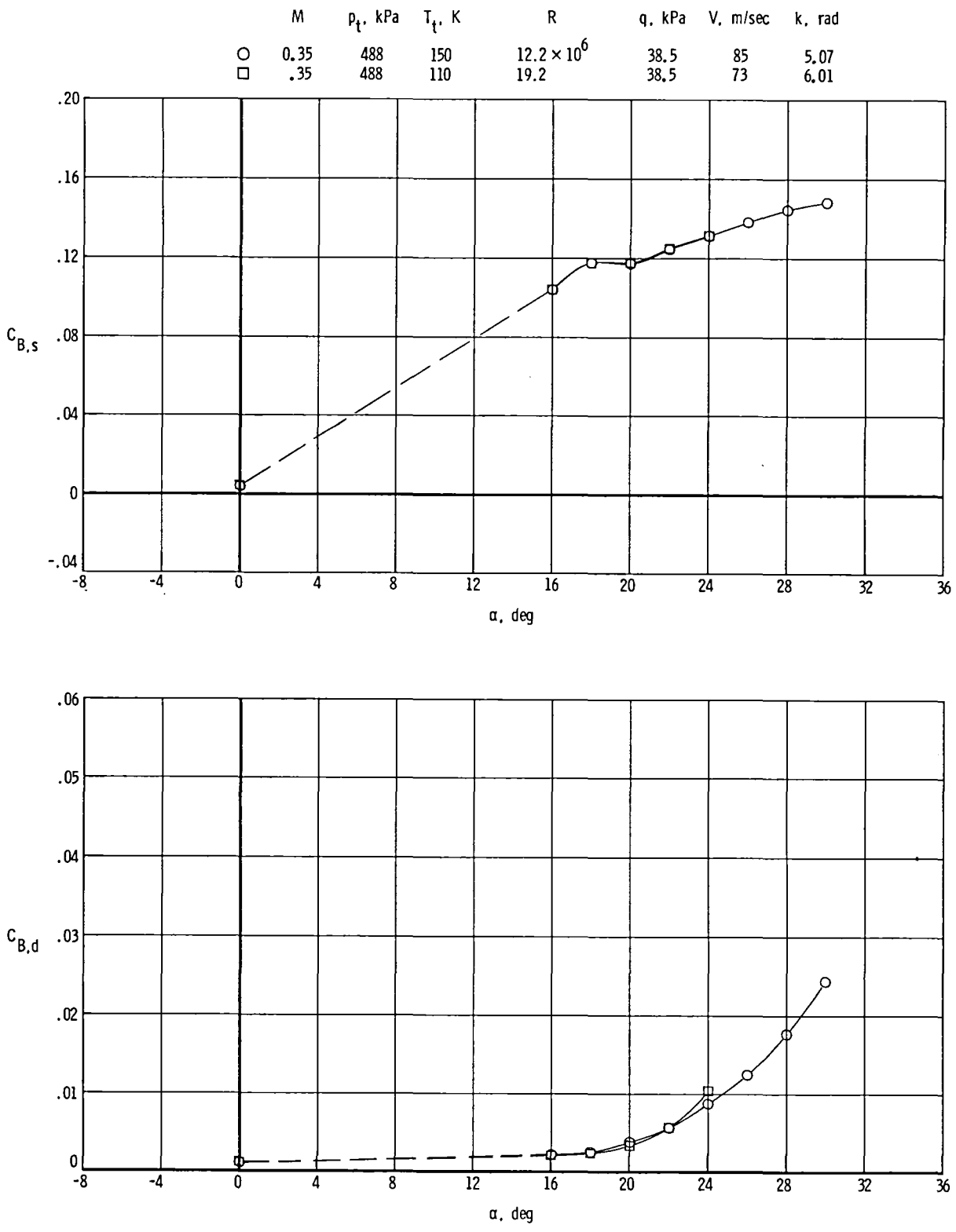

(e) M = 0.35; p_t = 488 kPa. Dashed line indicates interpolation based on other data.

Figure 8.- Continued.

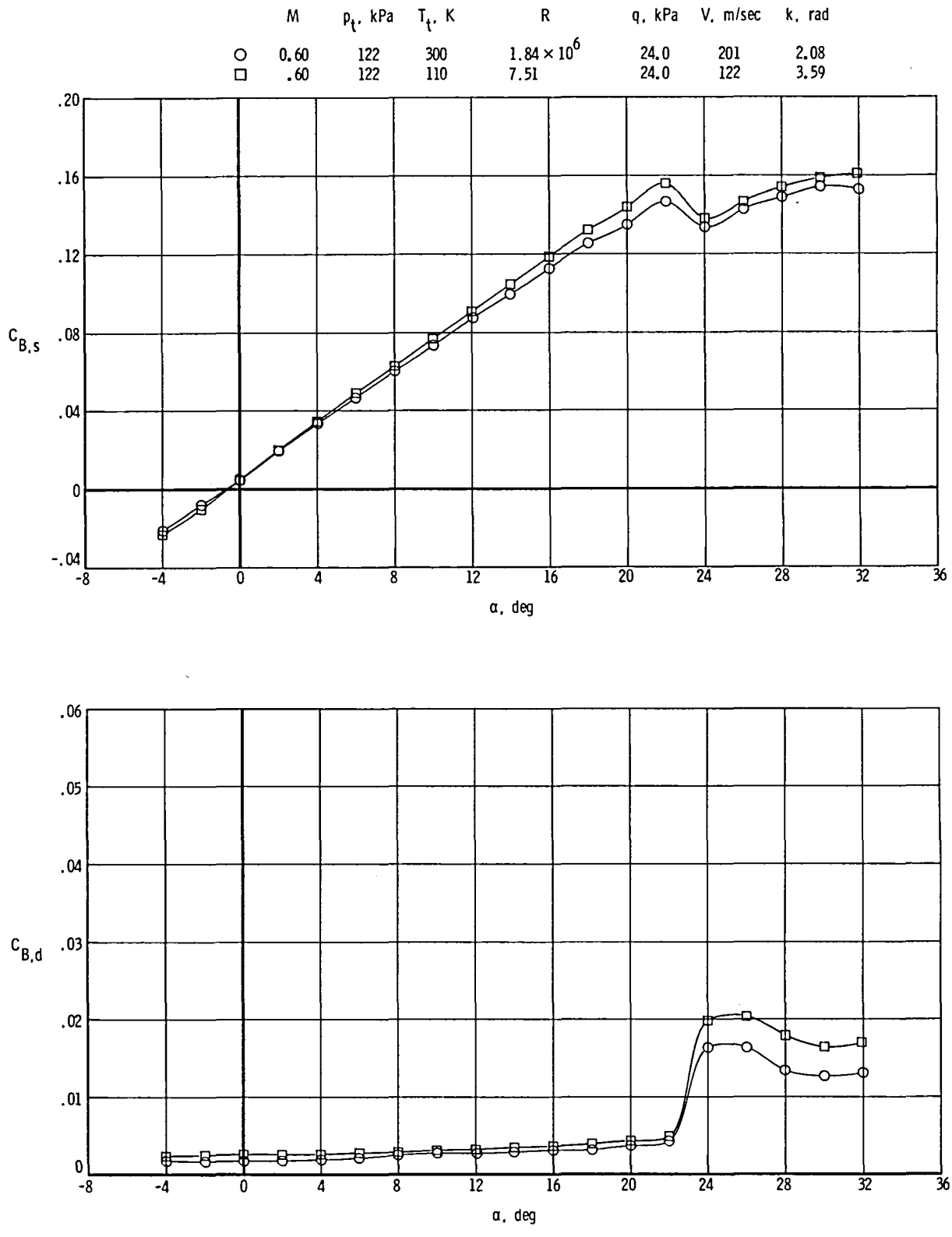

(f) M = 0.60; p_t = 122 kPa.

Figure 8.- Continued.

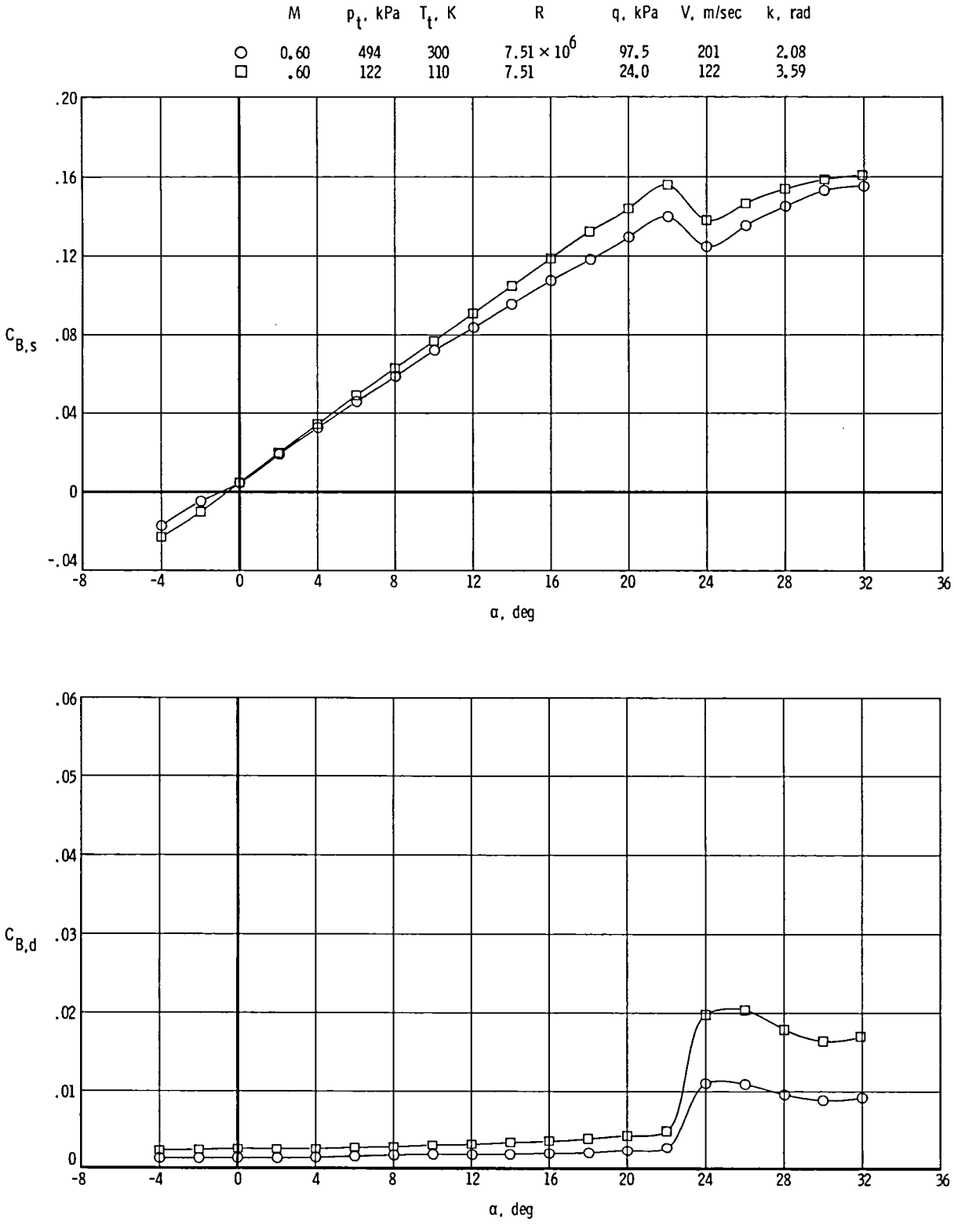

(g) M = 0.60; R = 7.51×10^6.

Figure 8.- Continued.

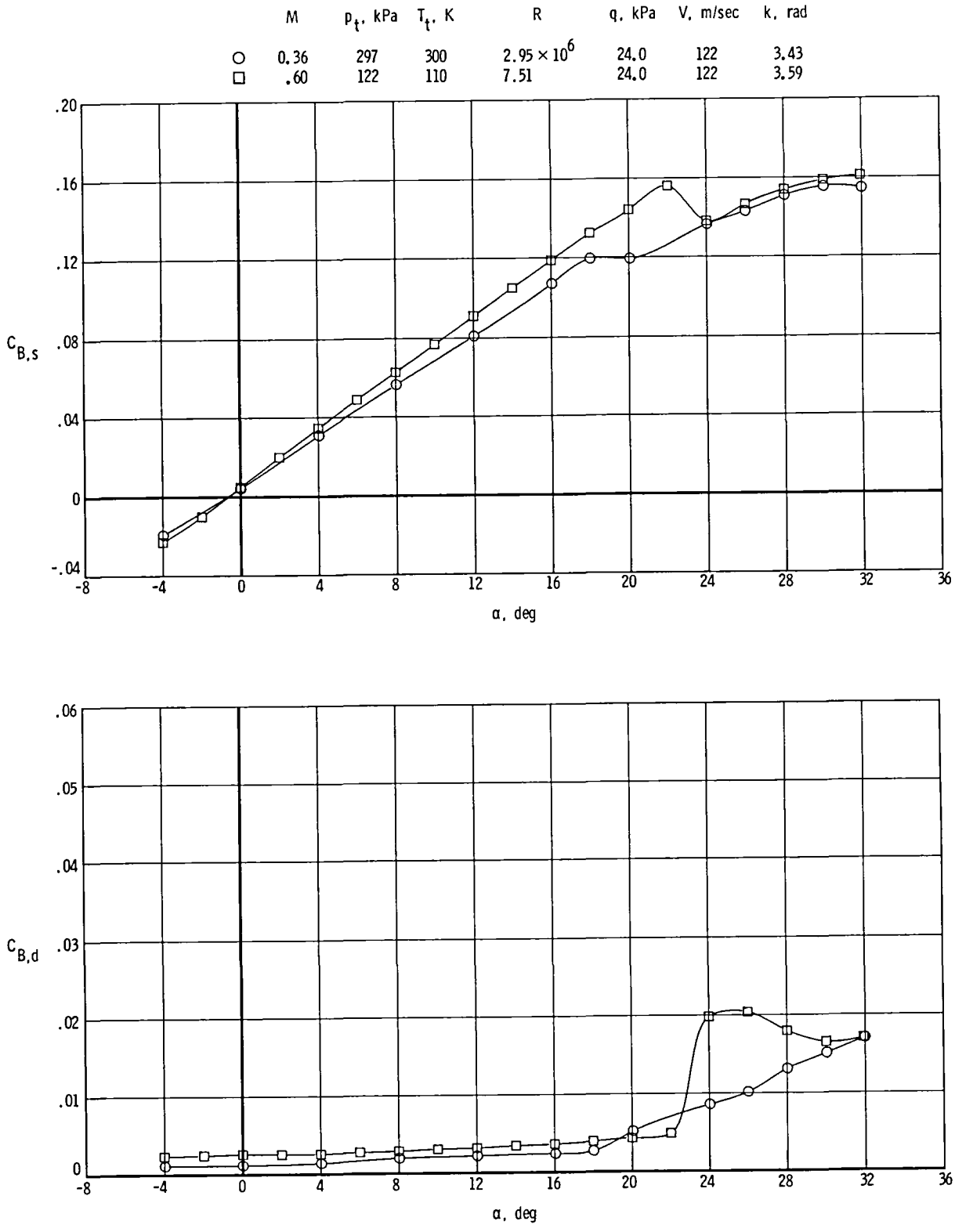

(h) V = 122 m/sec; q = 24.0 kPa.

Figure 8.- Continued.

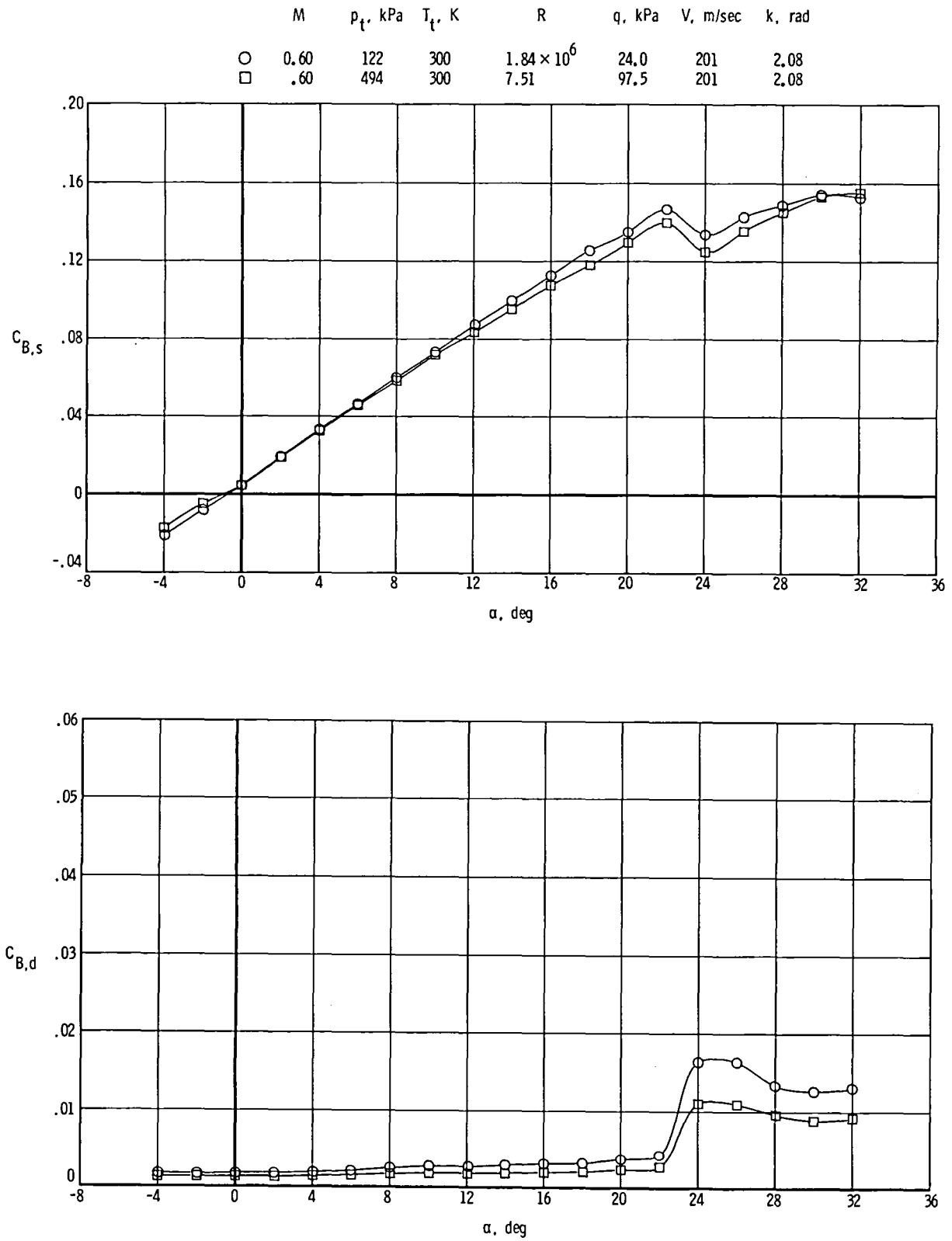

(i) M = 0.60; T_t = 300 K.

Figure 8.- Continued.

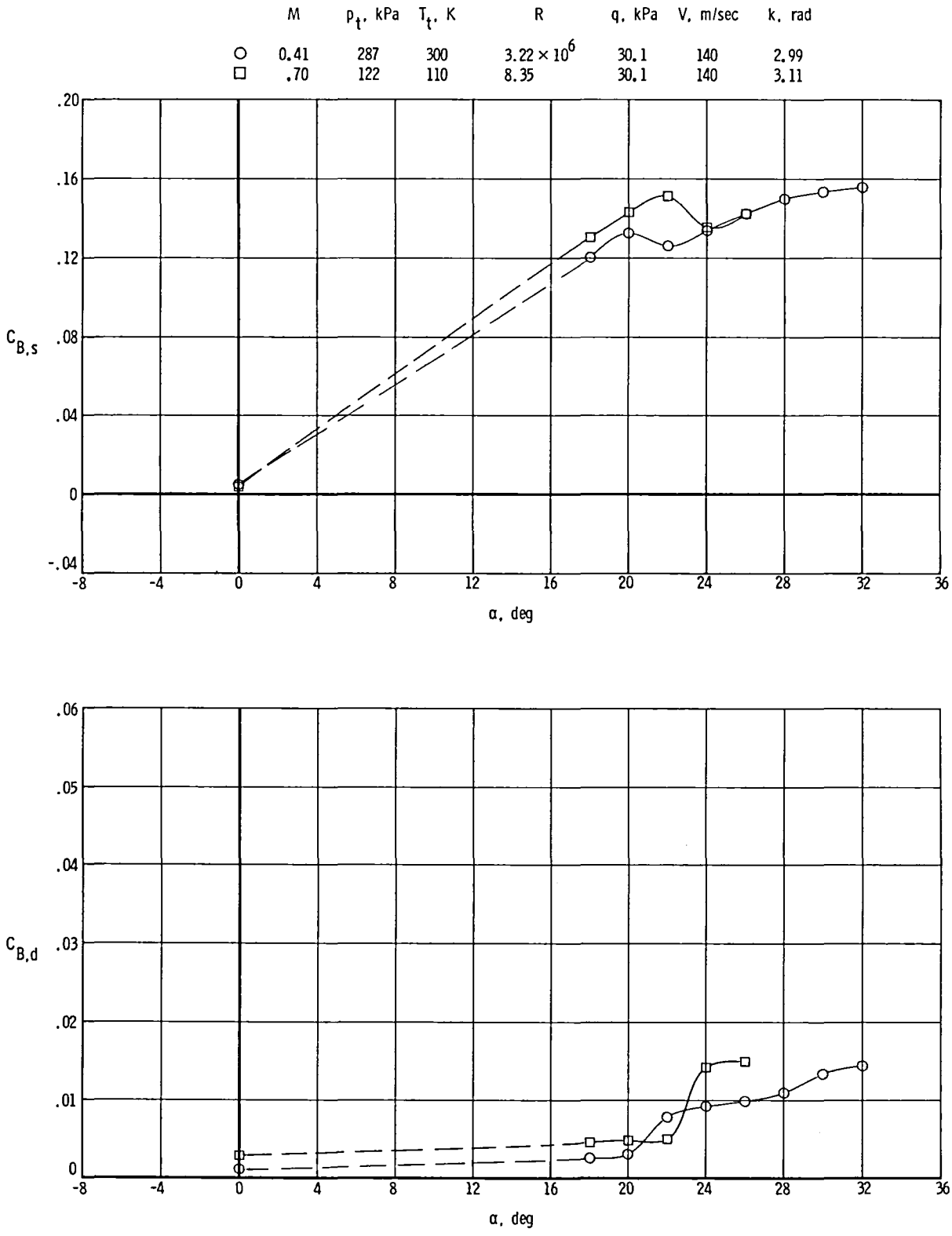

(j) V = 140 m/sec; q = 30.1 kPa. Dashed line indicates interpolation based on other data.

Figure 8.- Continued.

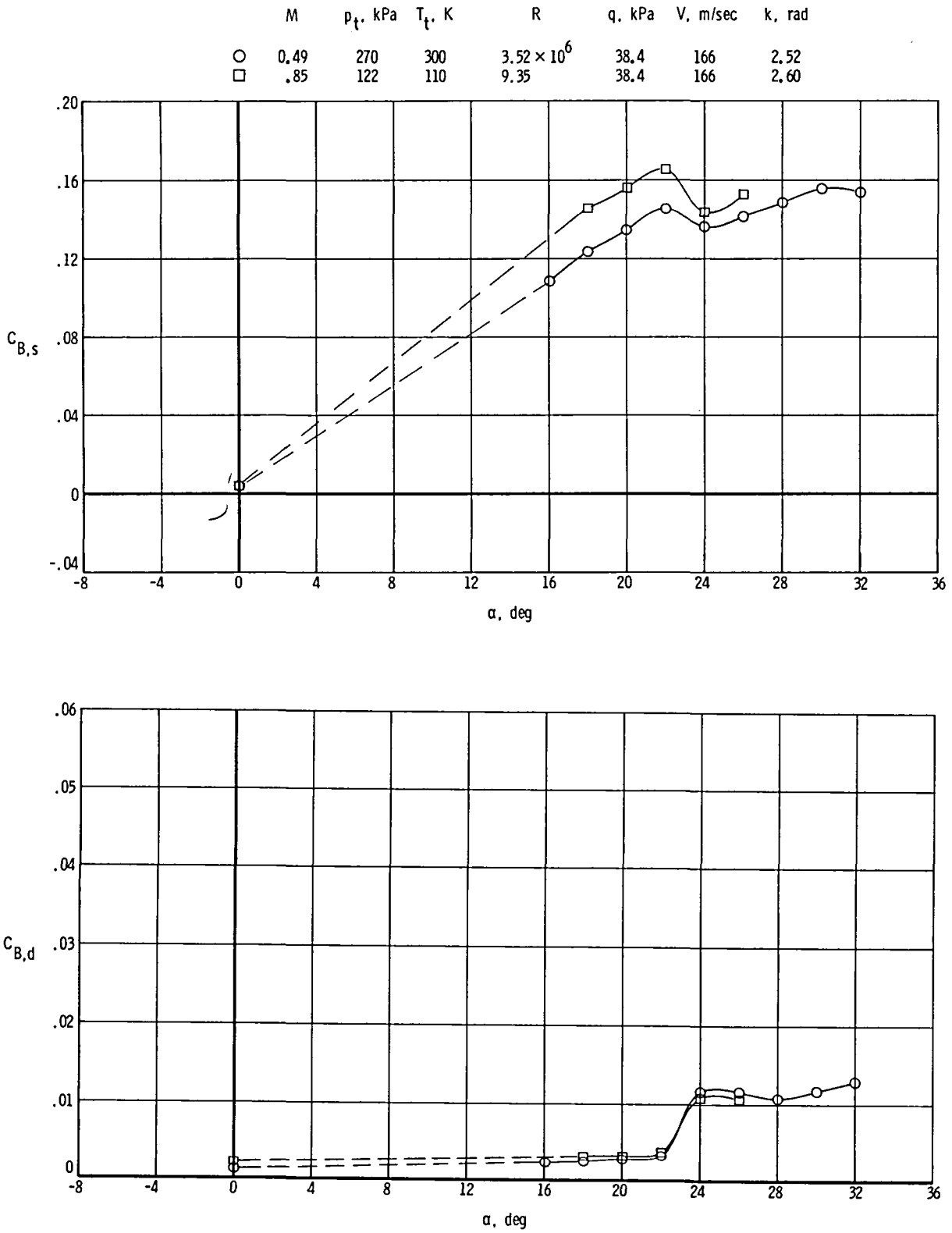

(k) V = 166 m/sec; q = 38.4 kPa. Dashed line indicates interpolation based on other data.

Figure 8.- Concluded.

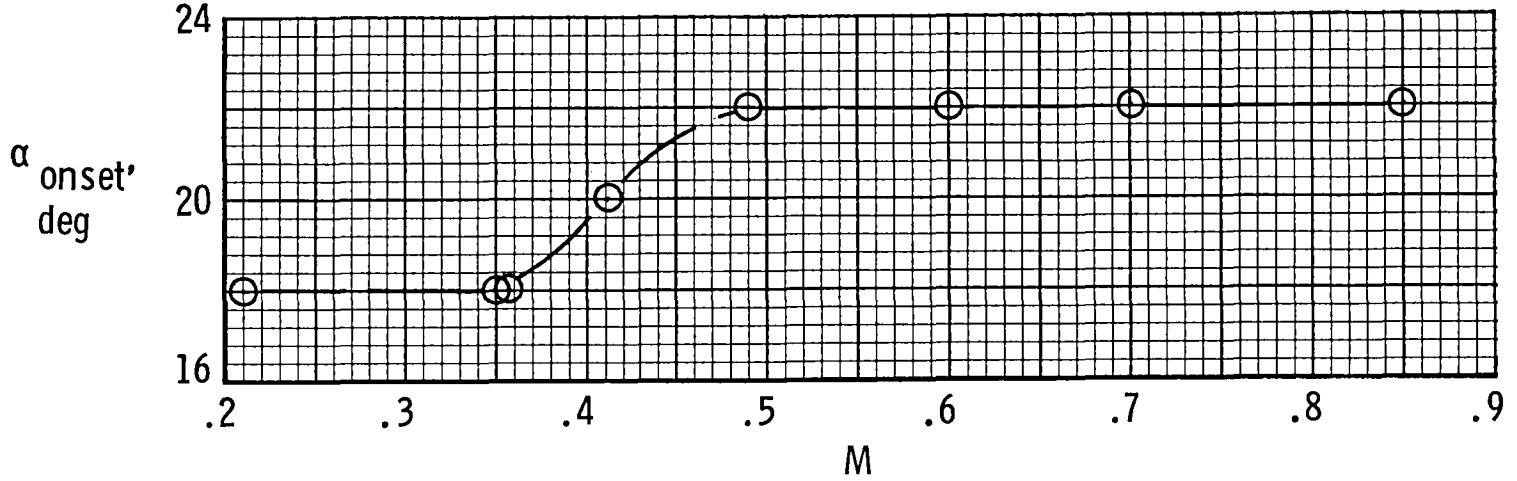

(a) Buffet-onset angle of attack.

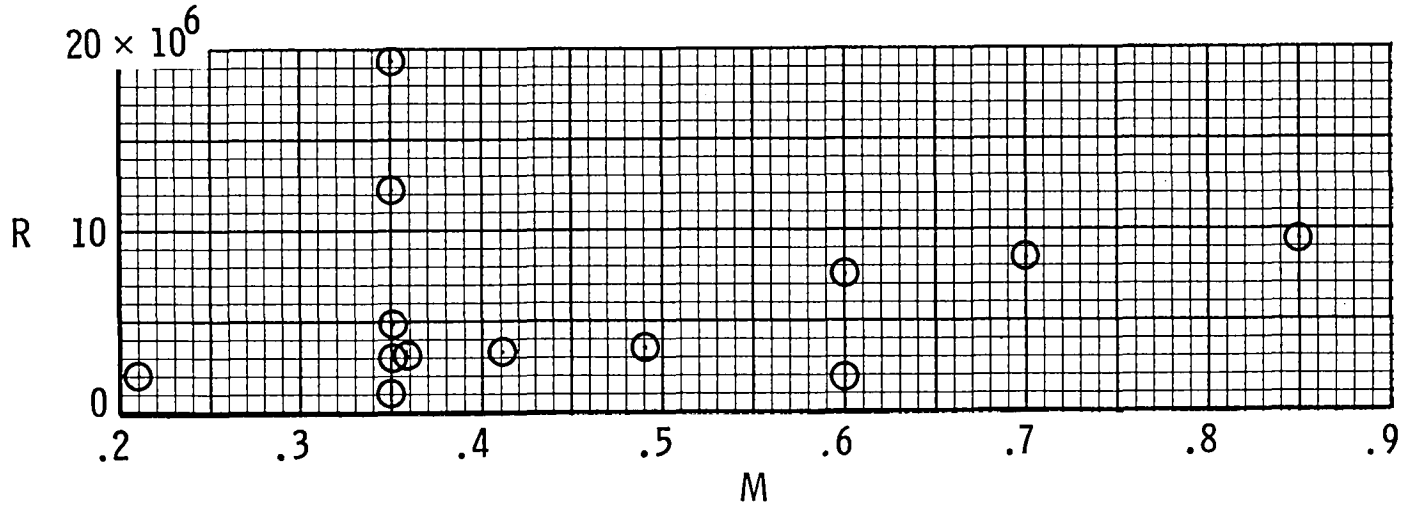

(b) Reynolds number range.

Figure 9.- Buffet-onset angle of attack and Reynolds number range for tests of delta-wing model.

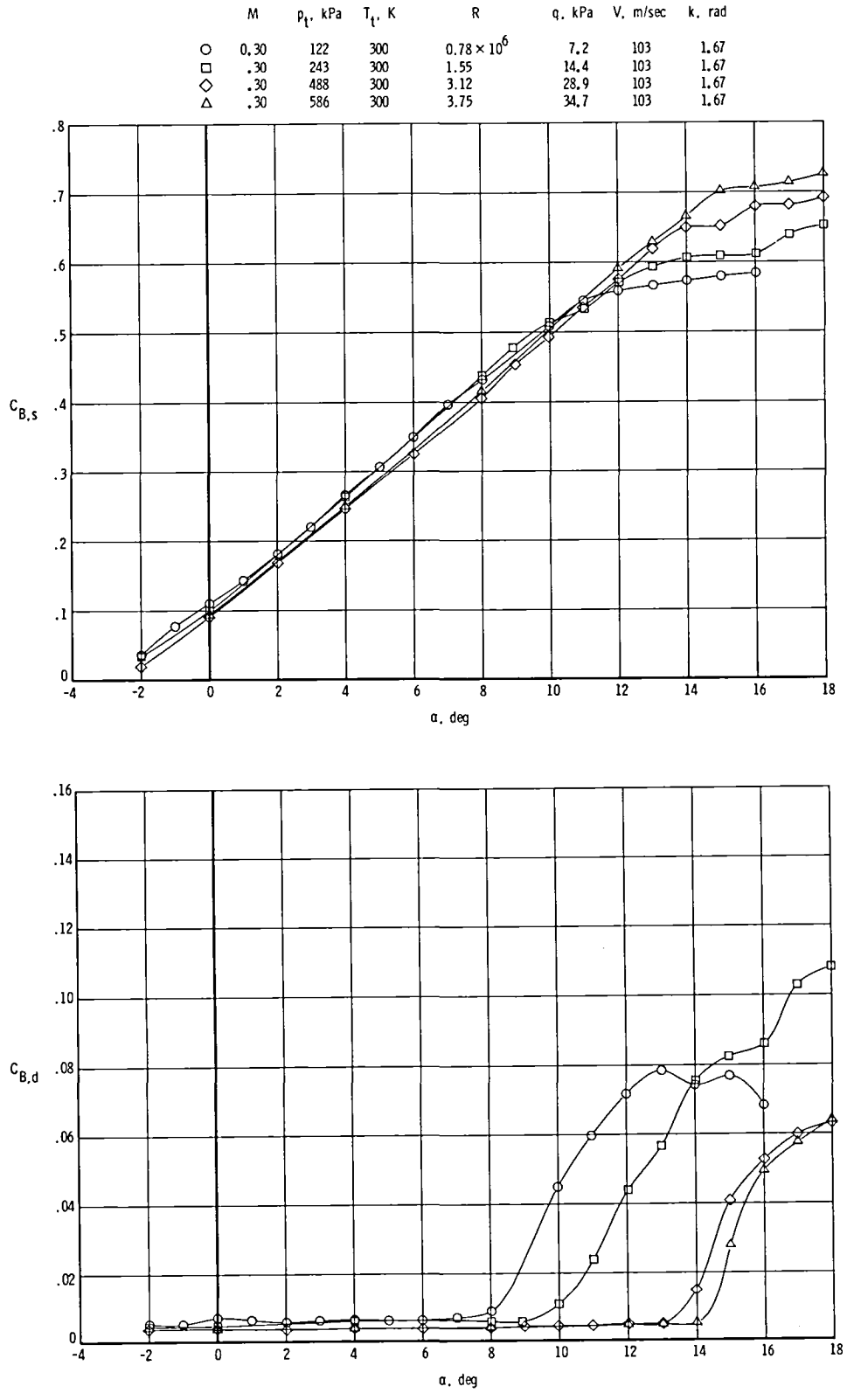

(a) M = 0.30; T_t = 300 K.

Figure 10.- Variation of steady and dynamic wing-root bending-moment coefficients with angle of attack for NPL 9510 wing model.

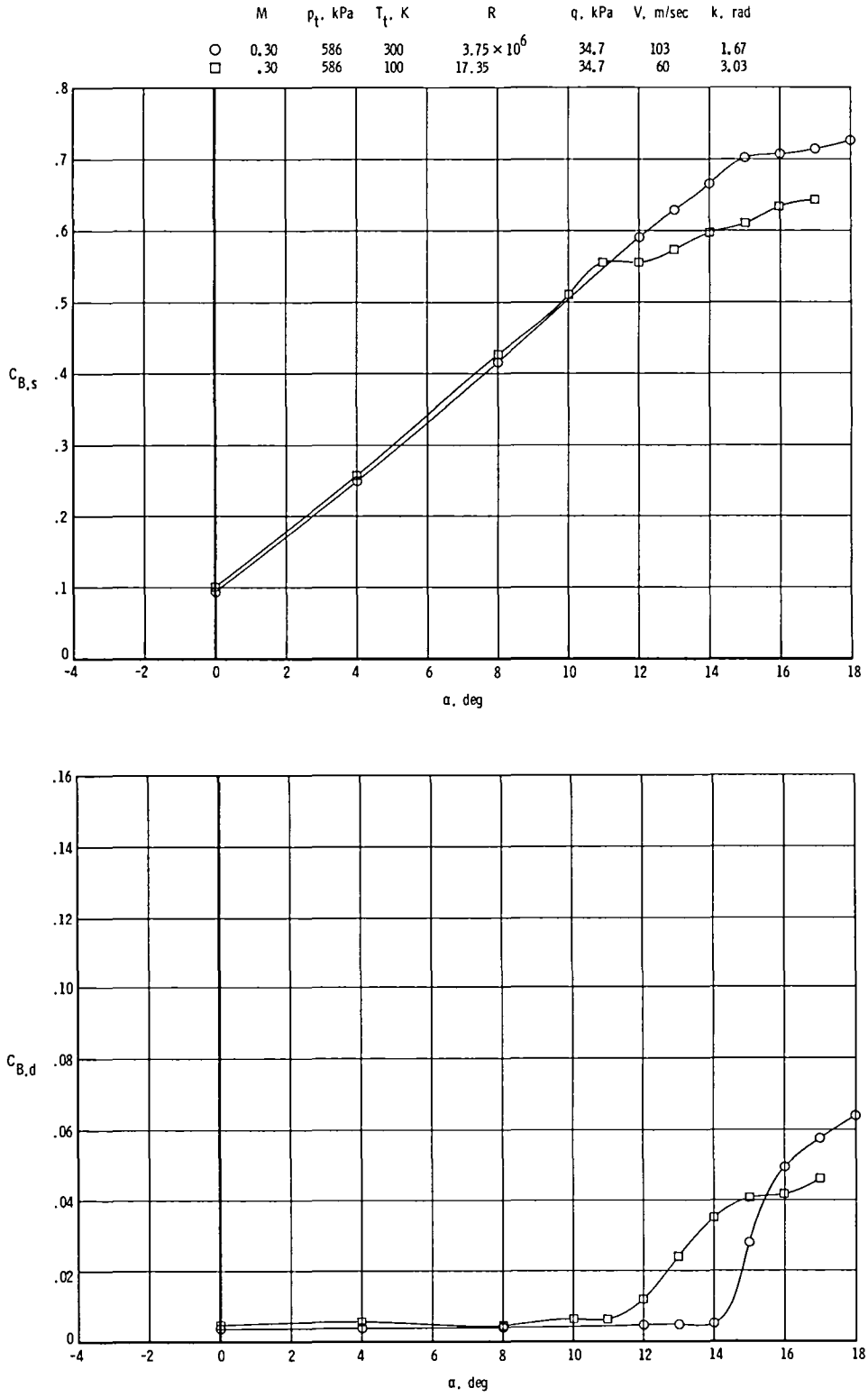

(b) M = 0.30; p_t = 586 kPa.

Figure 10.- Continued.

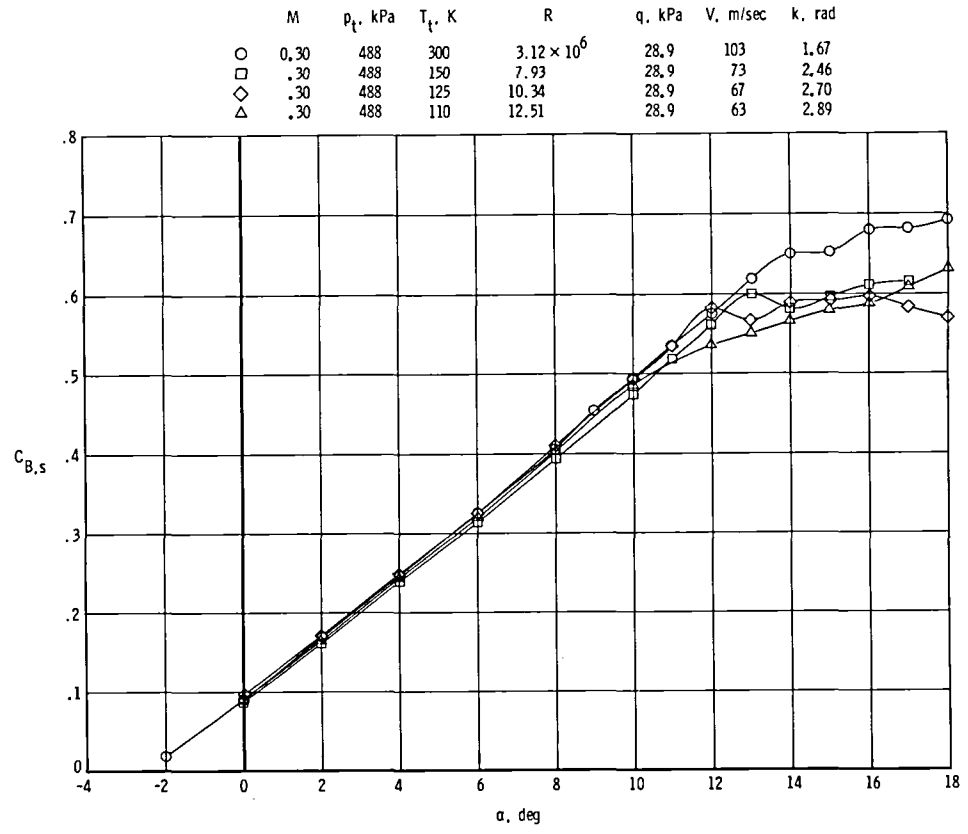

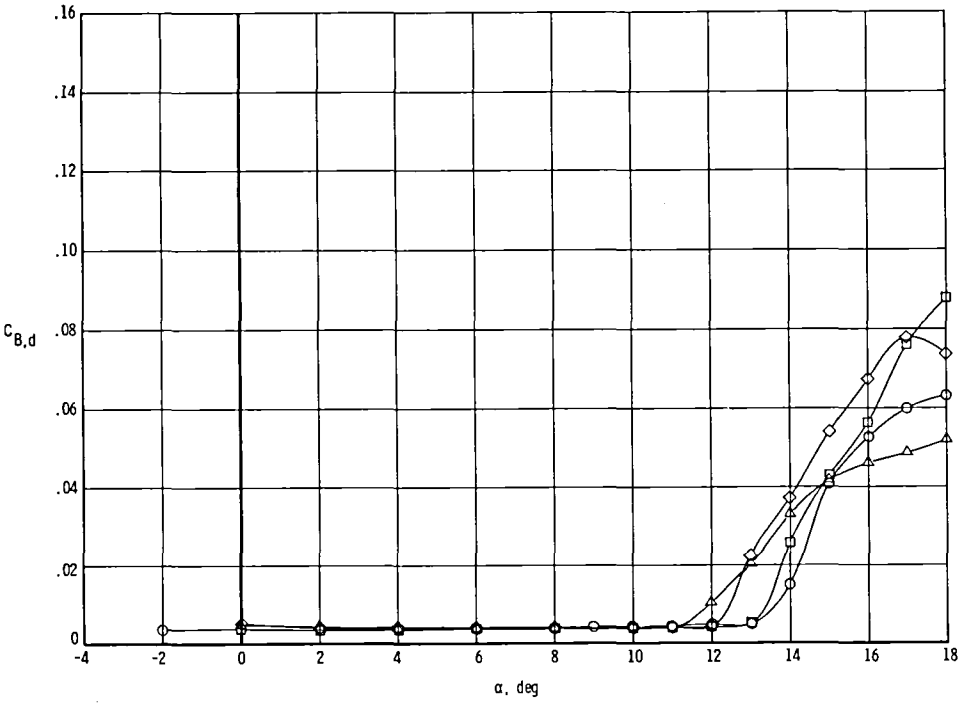

(c) M = 0.30; p_t = 488 kPa.

Figure 10.- Continued.

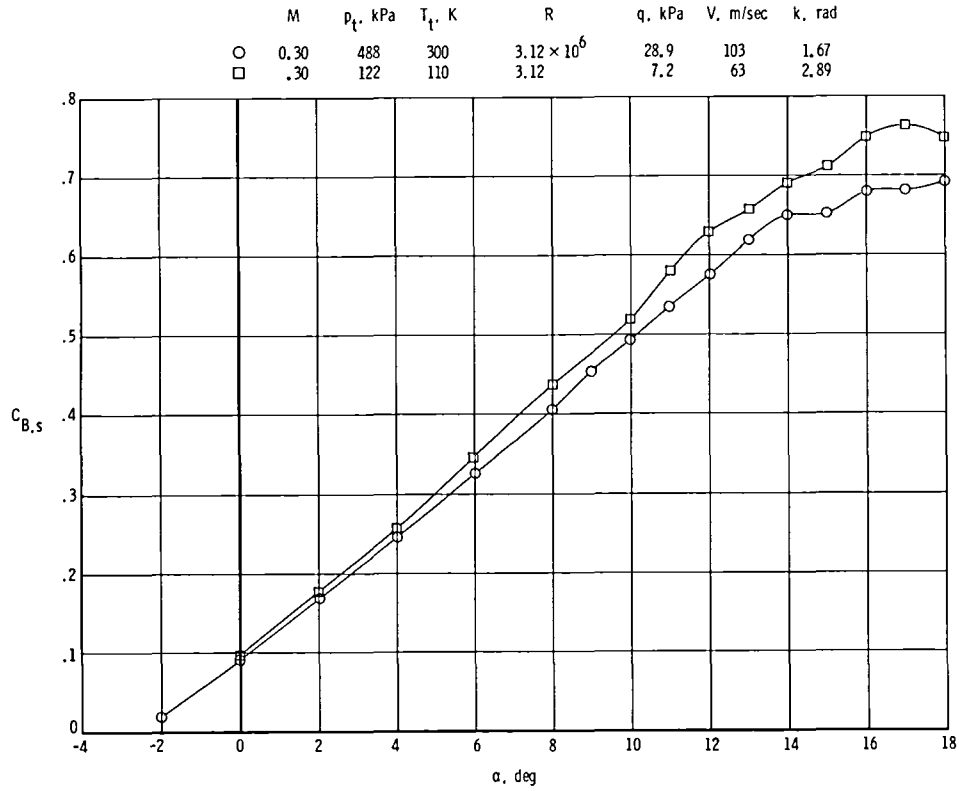

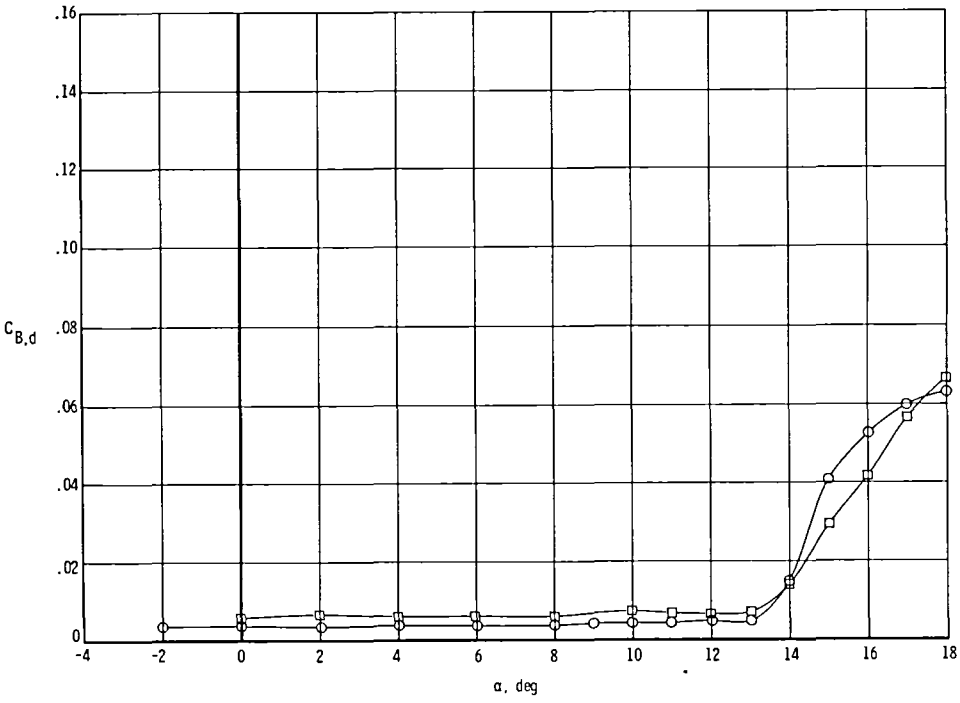

(d) M = 0.30; R = 3.12×10^6.

Figure 10.- Continued.

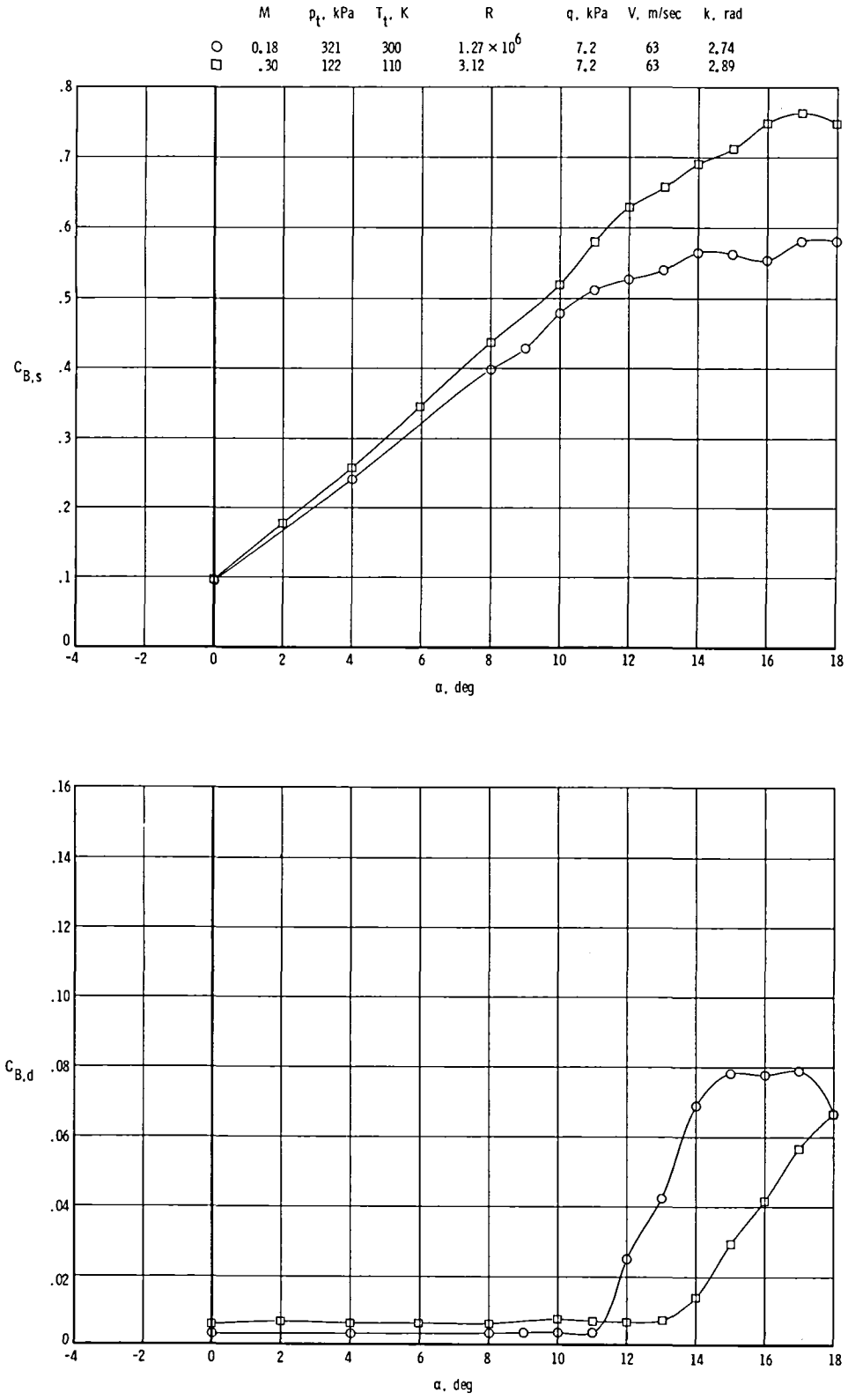

(e) V = 63 m/sec; q = 7.2 kPa.

Figure 10.- Continued.

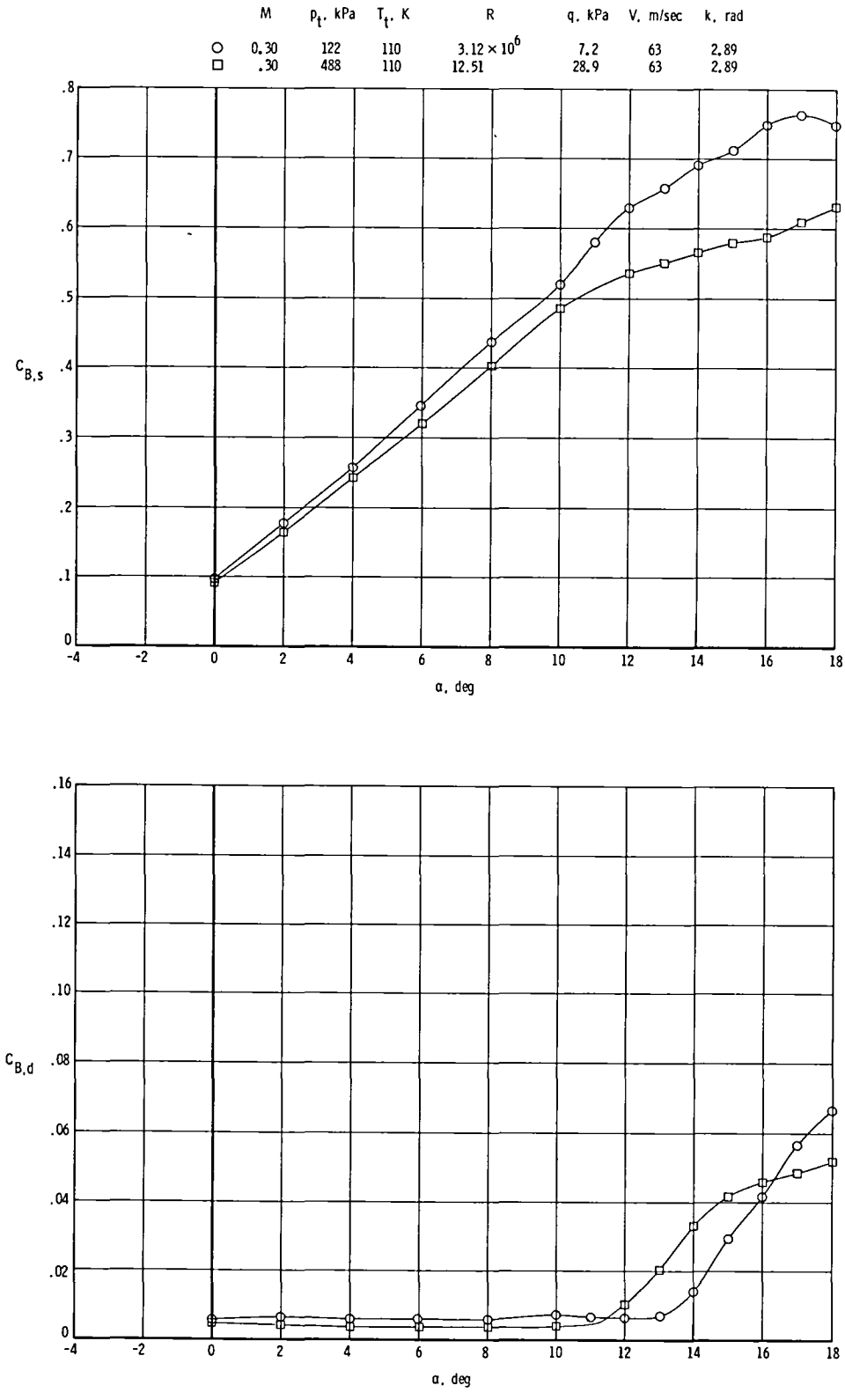

(f) M = 0.30; T_t = 110 K.

Figure 10.- Continued.

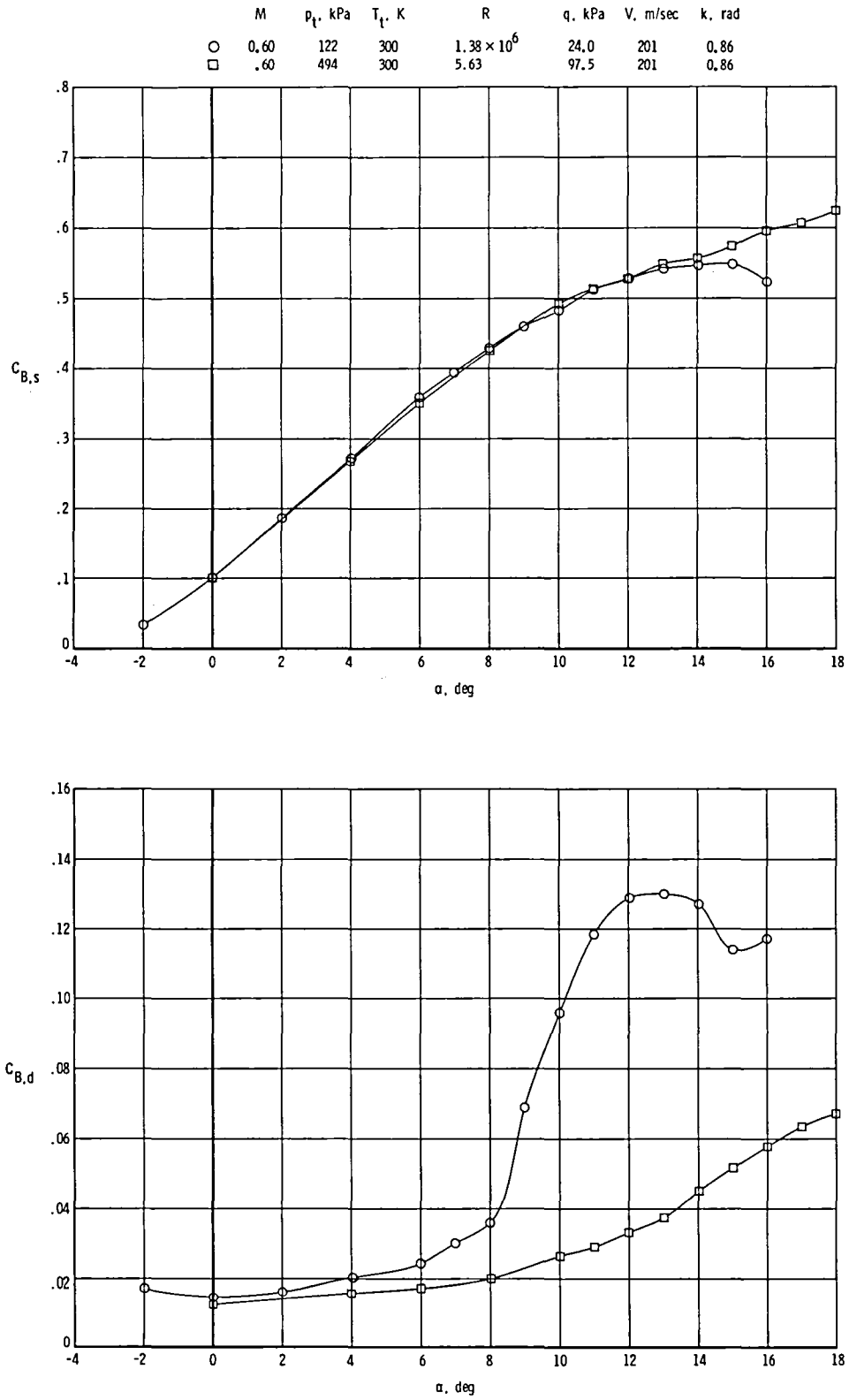

(g) M = 0.60; T_t = 300 K.

Figure 10.- Continued.

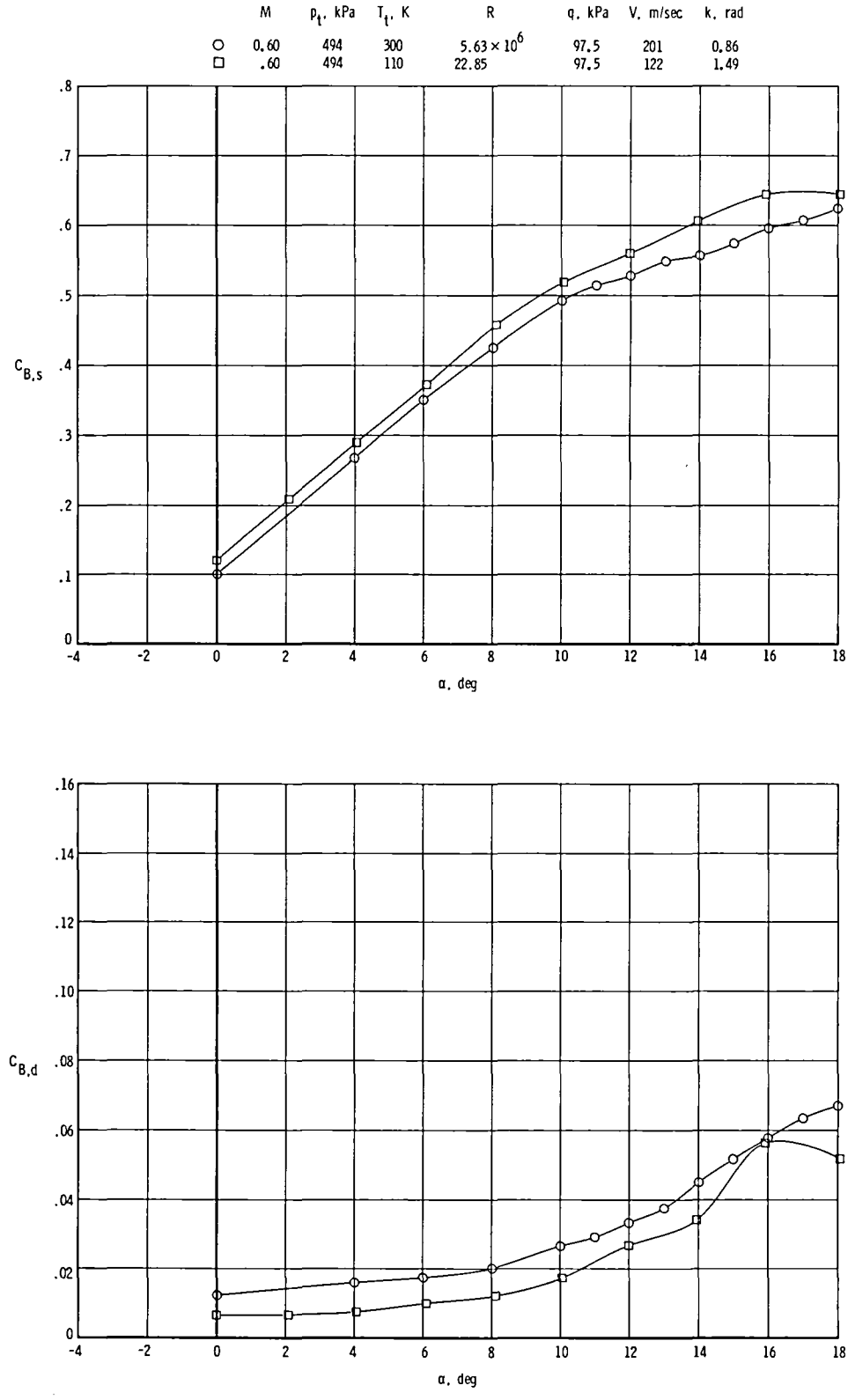

(h) M = 0.60; p_t = 494 kPa.

Figure 10.- Continued.

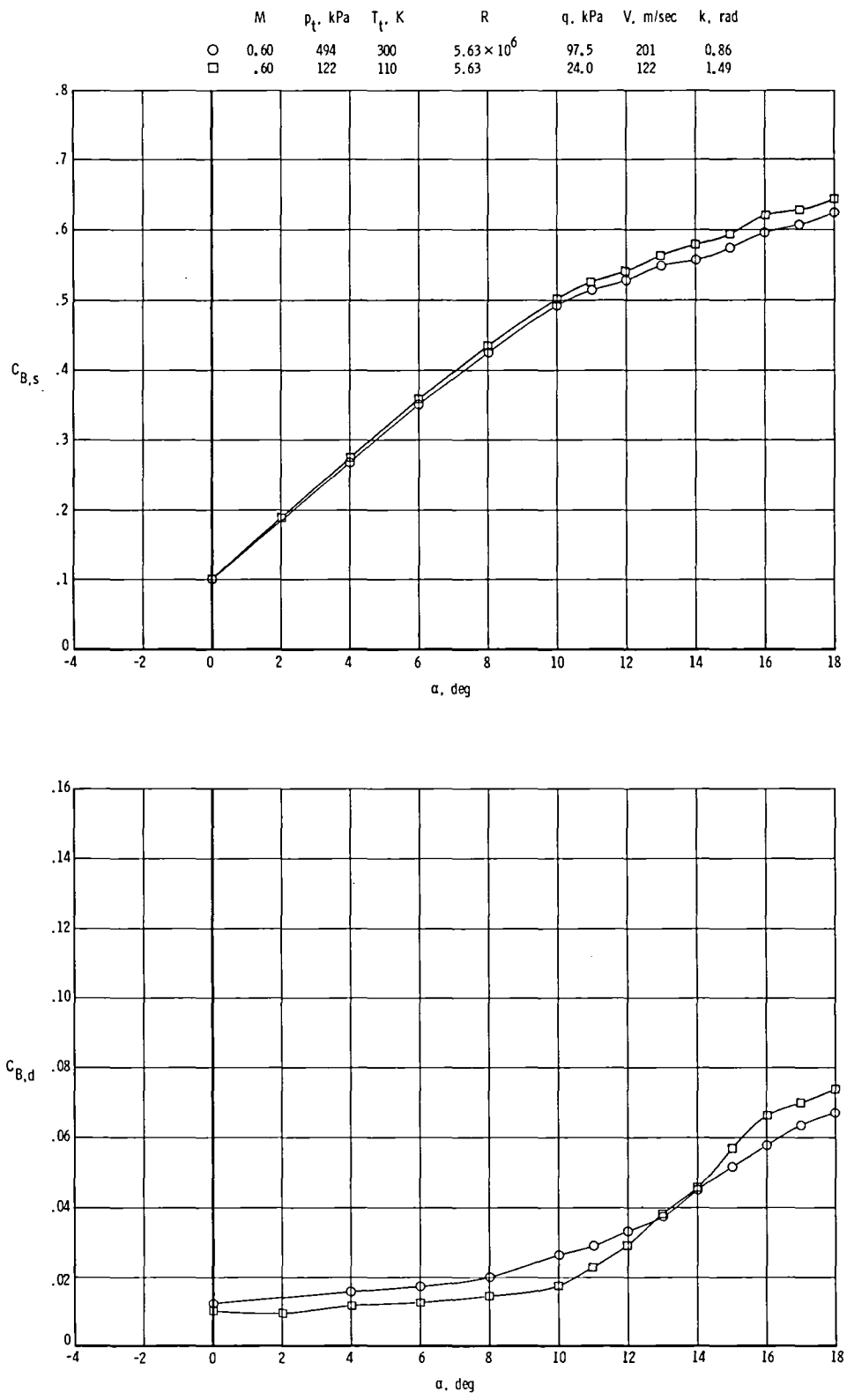

(i) M = 0.60; R = 5.63×10^6.

Figure 10.- Continued.

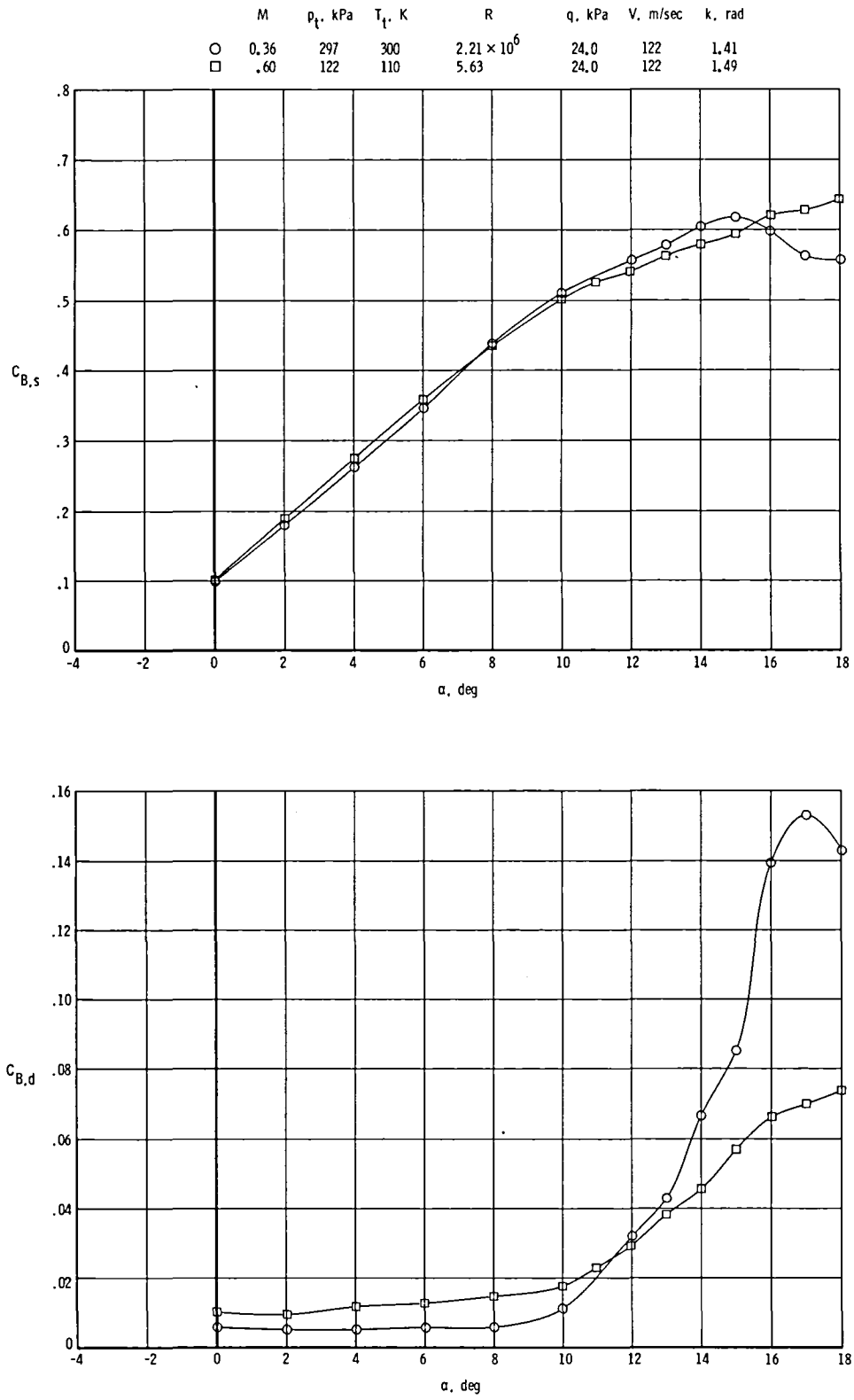

(j) V = 122 m/sec; q = 24.0 kPa.

Figure 10.- Continued.

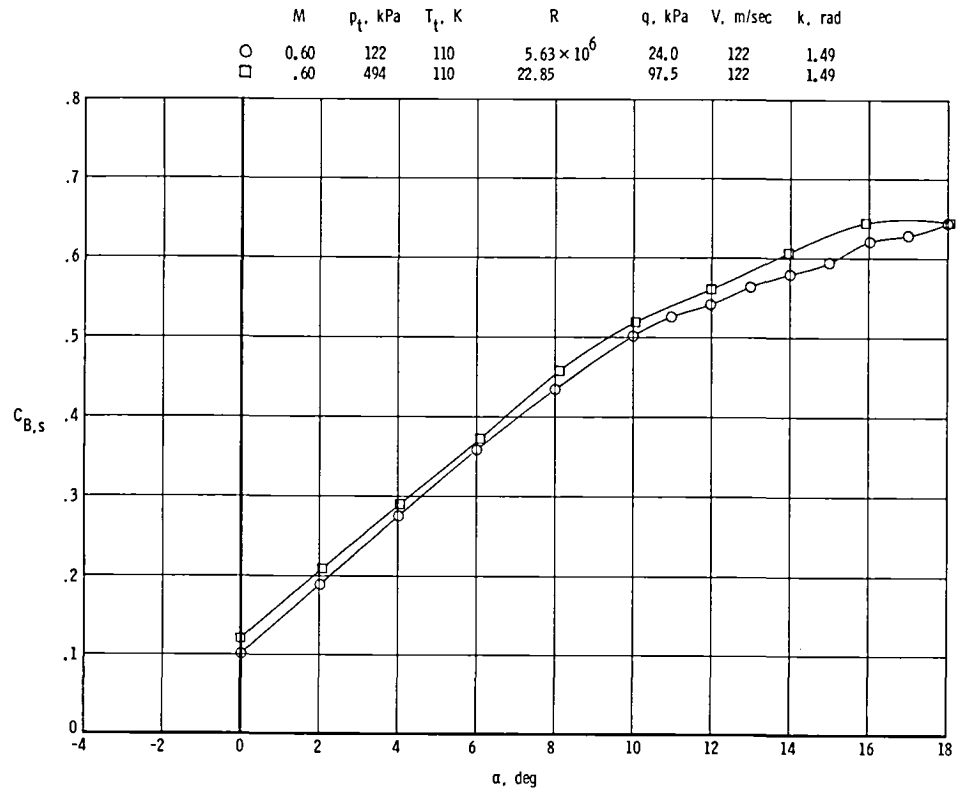

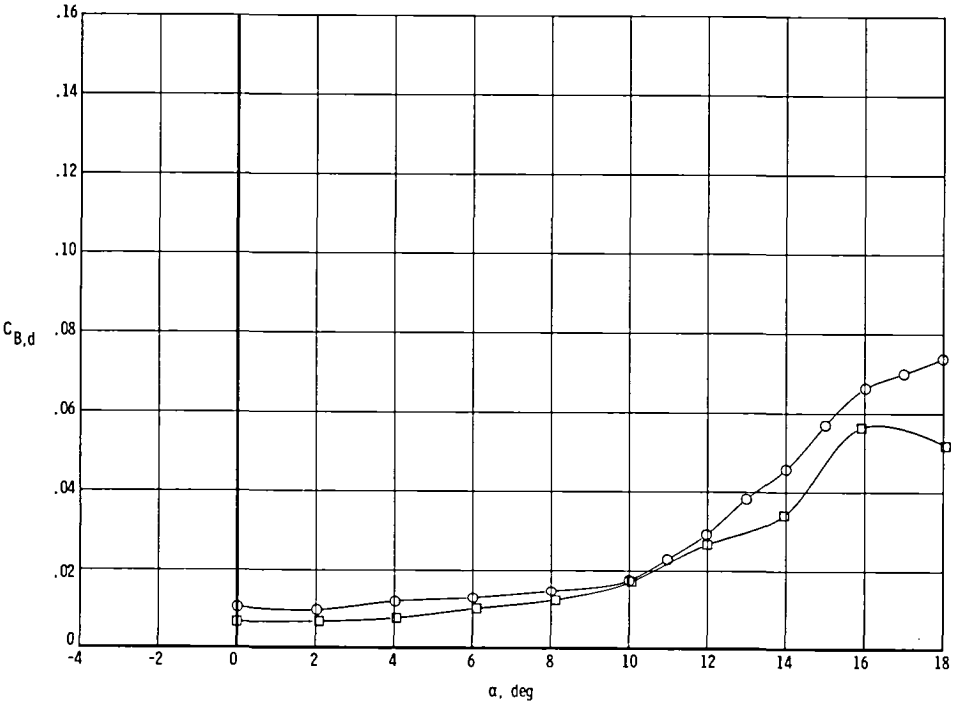

(k) M = 0.60; T_t = 110 K.

Figure 10.- Continued.

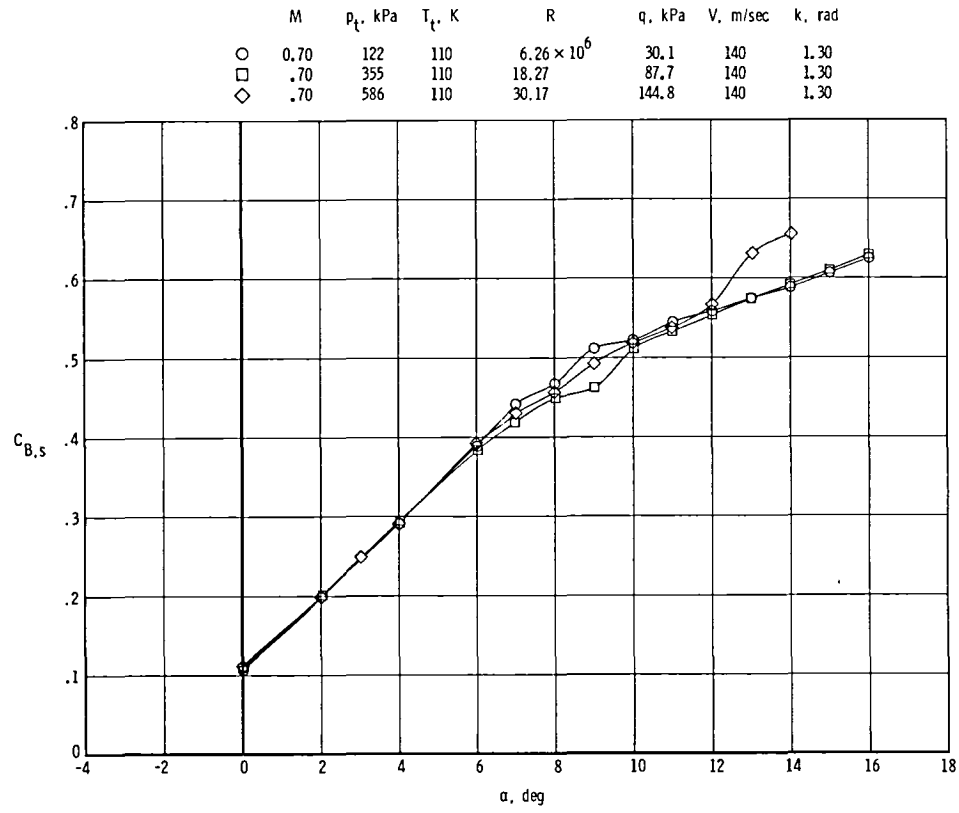

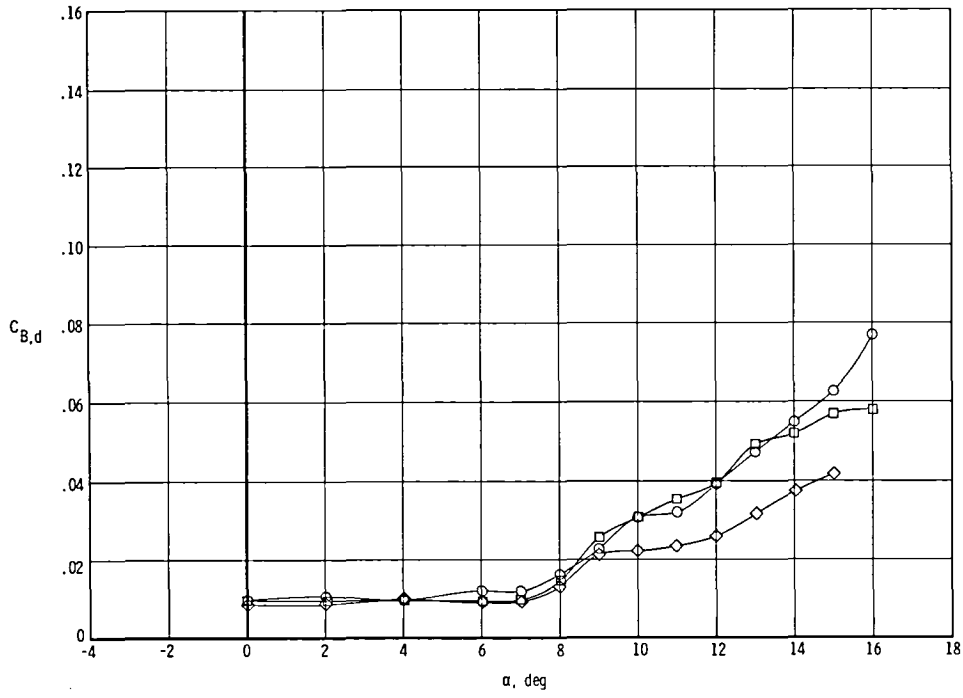

(l) M = 0.70; T_t = 110 K.

Figure 10.- Continued.

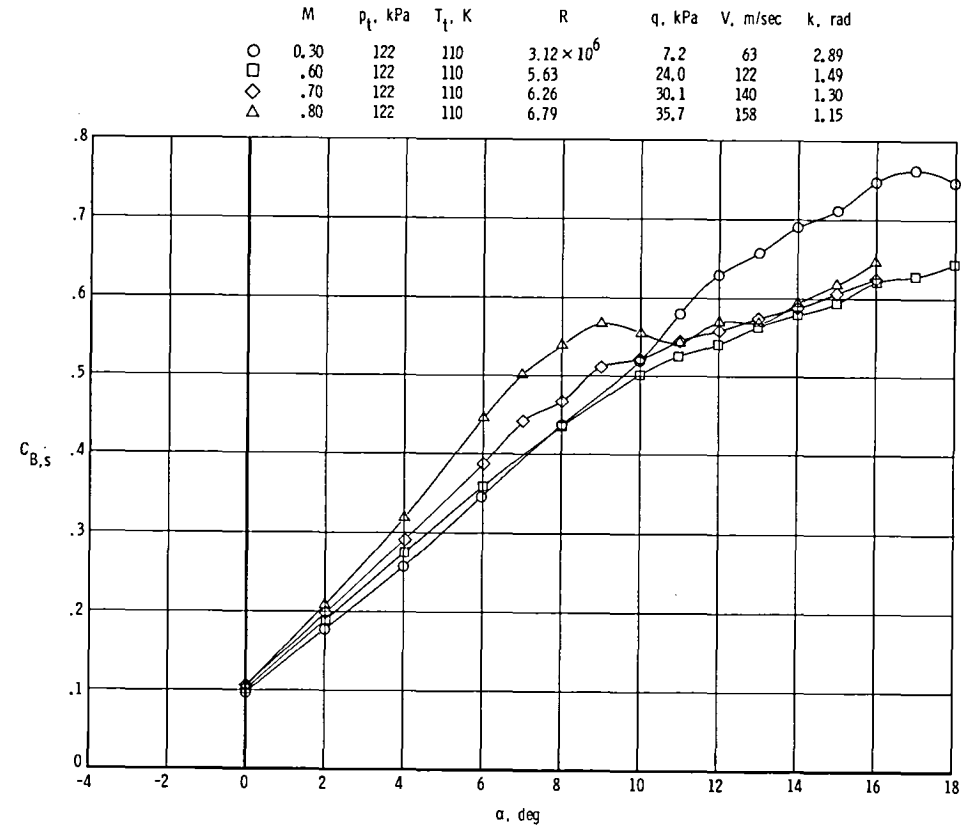

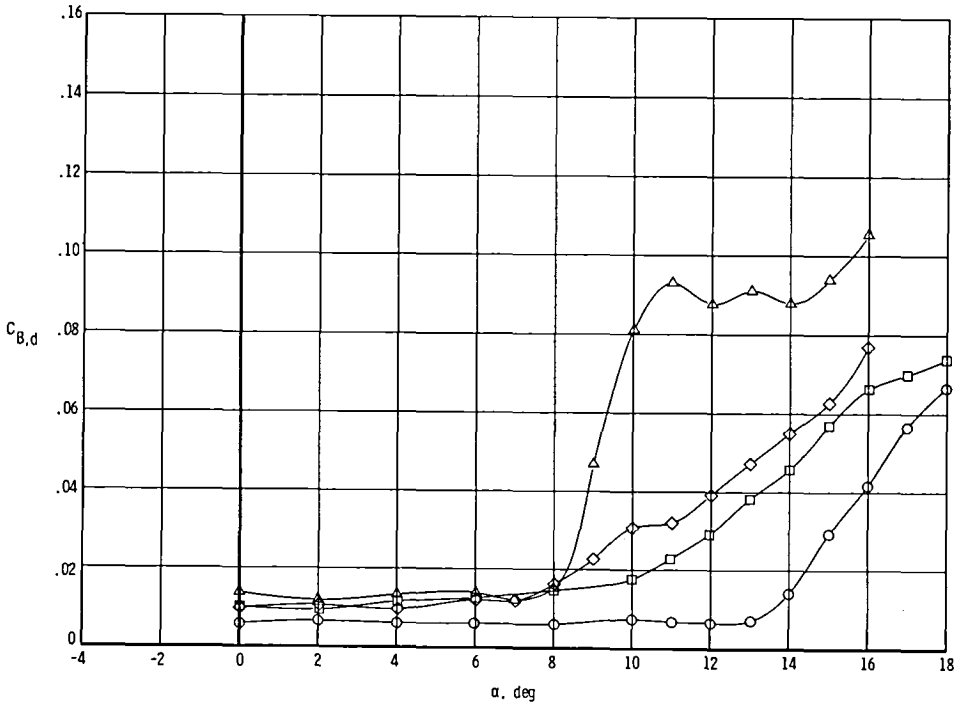

(m) p_t = 122 kPa; T_t = 110 K.

Figure 10.- Concluded.

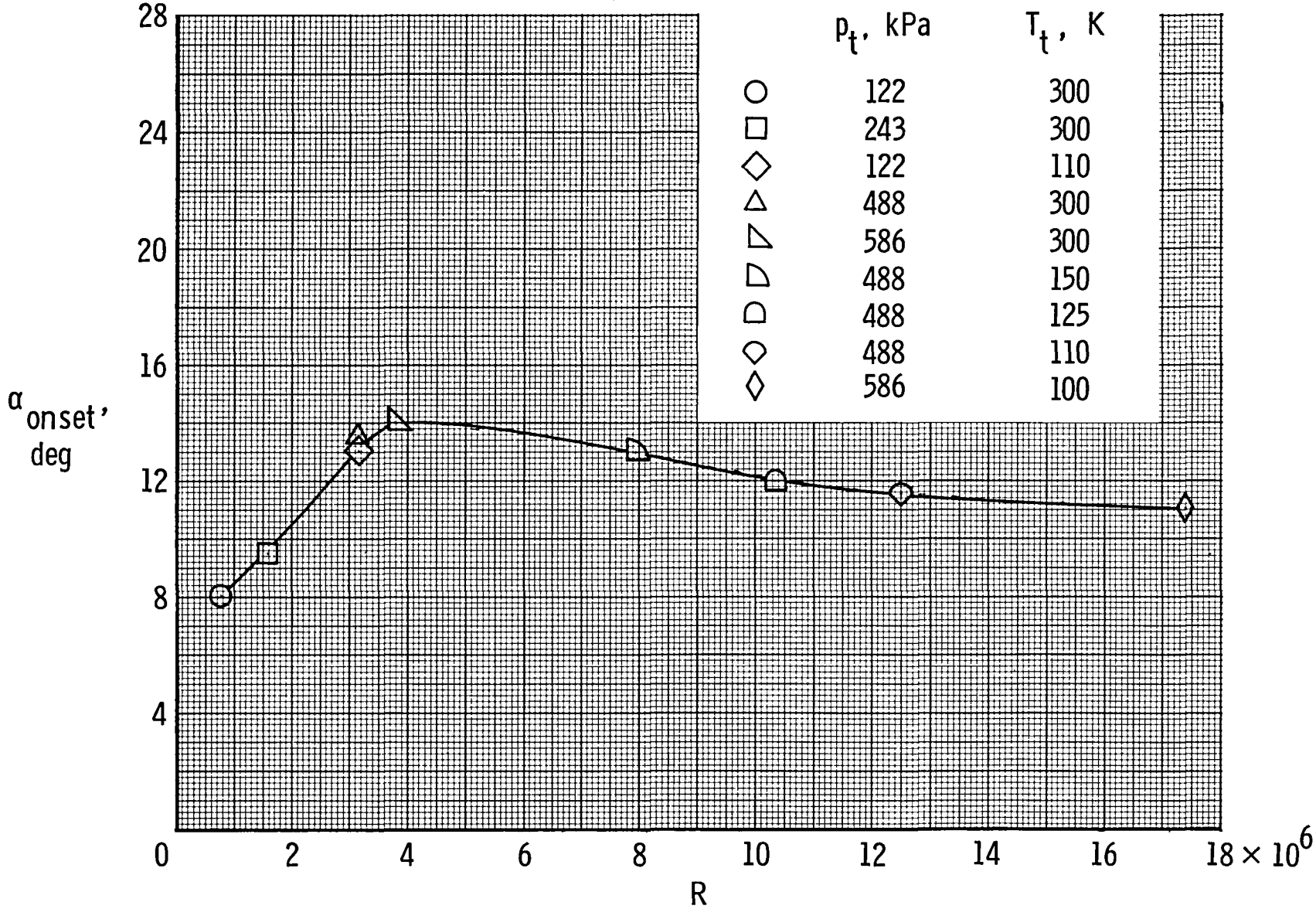

Figure 11.- Effect of Reynolds number on buffet-onset angle of attack for NPL 9510 wing model. M = 0.30.

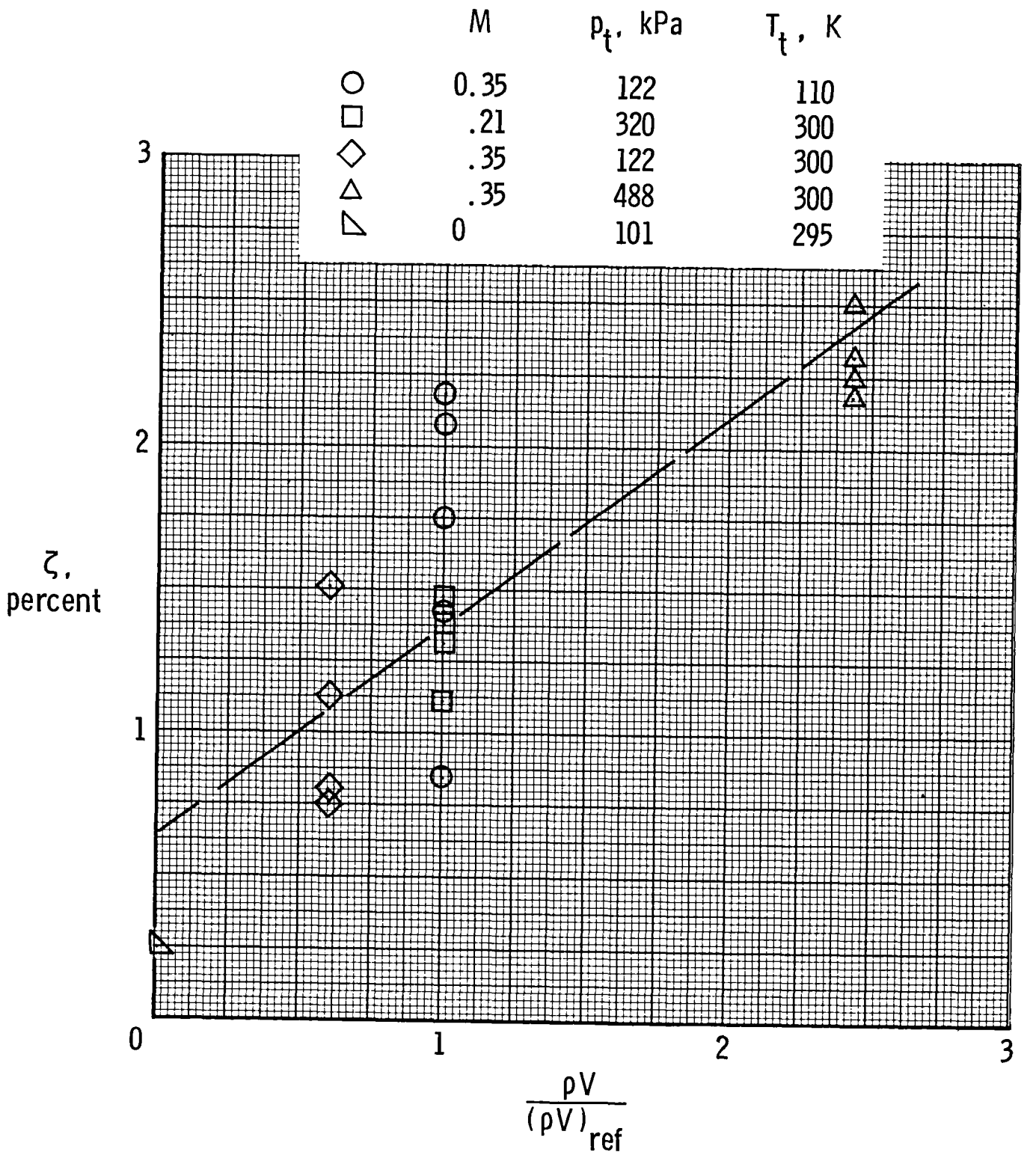

Figure 12.- Damping-ratio measurements for delta-wing model. $(\rho V)_{ref}$ denotes a reference condition at $M = 0.35$, $p_t = 122$ kPa, and $T_t = 110$ K.

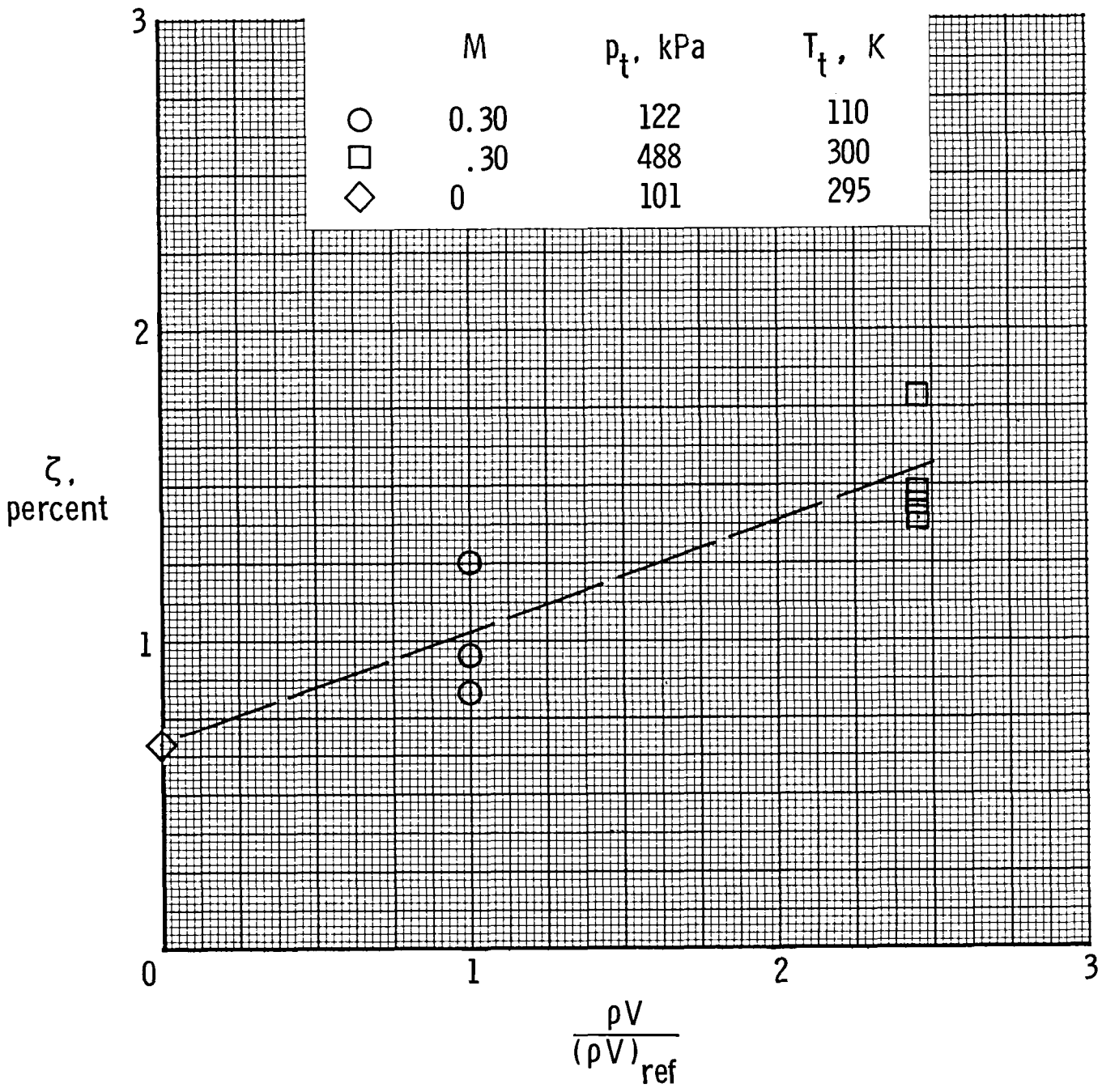

Figure 13.- Damping-ratio measurements for NPL 9510 wing model. $(\rho V)_{ref}$ denotes a reference condition at $M = 0.30$, $p_t = 122$ kPa, and $T_t = 110$ K.

1. Report No.	2. Government Accession No.	3. Recipient's Catalog No.
NASA TM-84520		

4. Title and Subtitle	5. Report Date
RESULTS OF BUFFET TESTS IN A CRYOGENIC WIND TUNNEL	September 1982
	6. Performing Organization Code: 505-31-53-06

7. Author(s)	8. Performing Organization Report No.
Richmond P. Boyden and William G. Johnson, Jr.	L-15370
	10. Work Unit No.

9. Performing Organization Name and Address	11. Contract or Grant No.
NASA Langley Research Center Hampton, VA 23665	
	13. Type of Report and Period Covered: Technical Memorandum

12. Sponsoring Agency Name and Address	14. Sponsoring Agency Code
National Aeronautics and Space Administration Washington, DC 20546	

15. Supplementary Notes

16. Abstract

Buffet tests on two semispan-wing models with different leading-edge sweep have shown that it is feasible to use the standard dynamic wing-root bending-moment technique in a cryogenic wind tunnel. One model was a slender 65°-swept delta wing with sharp leading edges. The other model was an unswept wing of aspect ratio 1.5 with a British NPL 9510 airfoil section. The results for the 65°-swept delta wing indicate the importance of matching the reduced-frequency parameter in model tests for planforms which are sensitive to reduced-frequency parameter if quantitative buffet measurements are required. The unique ability of a pressurized cryogenic wind tunnel to separate the effects of Reynolds number and of static aeroelastic distortion by variations in the tunnel stagnation temperature and pressure has been demonstrated.

17. Key Words (Suggested by Author(s))	18. Distribution Statement
Buffet tests Cryogenic wind tunnel	Unclassified - Unlimited Subject Category 02

19. Security Classif. (of this report)	20. Security Classif. (of this page)	21. No. of Pages	22. Price
Unclassified	Unclassified	49	A03

For sale by the National Technical Information Service, Springfield, Virginia 22161

NASA-Langley, 1982

National Aeronautics and
Space Administration

Washington, D.C.
20546

Official Business
Penalty for Private Use, $300

THIRD-CLASS BULK RATE

Postage and Fees Paid
National Aeronautics and
Space Administration
NASA-451

NASA

POSTMASTER: If Undeliverable (Section 158
Postal Manual) Do Not Return